NASA TN D-330

TECHNICAL NOTE

D-330

AERODYNAMIC PERFORMANCE AND STATIC STABILITY AT MACH NUMBER 3.3 OF AN AIRCRAFT CONFIGURATION EMPLOYING THREE TRIANGULAR WING PANELS AND A BODY OF EQUAL LENGTH

By Carlton S. James

Ames Research Center
Moffett Field, Calif.

NATIONAL AERONAUTICS AND SPACE ADMINISTRATION

WASHINGTON August 1960

NATIONAL AERONAUTICS AND SPACE ADMINISTRATION

TECHNICAL NOTE D-330

AERODYNAMIC PERFORMANCE AND STATIC STABILITY AT MACH NUMBER 3.3 OF AN AIRCRAFT CONFIGURATION EMPLOYING THREE TRIANGULAR WING PANELS AND A BODY OF EQUAL LENGTH

By Carlton S. James

SUMMARY

An aircraft configuration, previously conceived as a means to achieve favorable aerodynamic stability characteristics, high lift-drag ratio, and low heating rates at high supersonic speeds, was modified in an attempt to increase further the lift-drag ratio without adversely affecting the other desirable characteristics. The original configuration consisted of three identical triangular wing panels symmetrically disposed about an ogive-cylinder body equal in length to the root chord of the panels. This configuration was modified by altering the angular disposition of the wing panels, by reducing the area of the panel forming the vertical fin, and by reshaping the body to produce interference lift.

Six-component force and moment tests of the modified configuration at combined angles of attack and sideslip were made at a Mach number of 3.3 and a Reynolds number of 5.46 million. A maximum lift-drag ratio of 6.65 (excluding base drag) was measured at a lift coefficient of 0.100 and an angle of attack of 3.6°. The lift-drag ratio remained greater than 3 up to lift coefficient of 0.35. Performance estimates, which predicted a maximum lift-drag ratio for the modified configuration 27 percent greater than that of the original configuration, agreed well with experiment.

The modified configuration exhibited favorable static stability characteristics within the test range. Longitudinal and directional centers of pressure were slightly aft of the respective centroids of projected plan-form and side area.

INTRODUCTION

On the basis of a theoretical study of factors influencing flight range and aerodynamic heating at high speeds, a configuration for a hypersonic glide vehicle was described and evaluated theoretically in reference 1. This configuration consists of a rotationally symmetrical placement of three half-delta wing panels about an ogive-cylinder body of circular cross section and of length equal to the root chord of the wing panels. From the standpoint of inherent aerodynamic stability, high aerodynamic efficiency, low heating rates, and acceptable low-speed performance, the configuration appears attractive also as a supersonic cruise airplane. Experimental measurements of the aerodynamic characteristics of a slightly modified version at low speed (references 2 and 3) have demonstrated favorable static stability characteristics and reasonable performance at landing speeds and attitudes. In reference 4 the longitudinal characteristics of a shortened version having large leading-edge bluntness were measured at Mach numbers from 3.00 to 6.28. Static longitudinal stability was shown to be favorable throughout the speed range, while performance appeared to suffer significantly from the wave drag associated with leading-edge bluntness and the loss in wing area (relative to body frontal area) due to shortening.

A 3 2 8

In the present study, a further evaluation of the design concept of reference 1 is carried out at a Mach number of 3.30. The specific purpose of the present study is to make a number of intuitively conceived modifications to the design of reference 1 in an attempt to improve its aerodynamic performance while retaining the inherent stability characteristics of the original design, and to determine experimentally the resulting performance and static stability of the modified configuration.

NOTATION

All moments are taken about the center of gravity of the model which is located on the model axis at the quarter point of the mean aerodynamic chord. This point is at the mid-length of the model. The model axis is defined as the line in the plane of symmetry of the model lying parallel to and 0.238 inch (3.29 percent l) below the intersection of the center planes of the three wing panels. Symbols are defined as follows:

A_{max}	maximum cross-sectional area of body
A_b	total base area of wings and body
b	wing span (twice the distance from model axis to wing tip)
$\bar{c}$	mean aerodynamic chord of wing

C_A	axial-force coefficient, $\frac{\text{axial force}}{qS}$
C_{A_b}	coefficient of axial force due to base pressure, $\frac{(p_b - p_\infty)A_b}{qS}$
C_D	drag coefficient, $\frac{D}{qS}$
$C_{D_{fore}}$	drag coefficient when $p_b = p_\infty$ (i.e., when base drag is zero)
C_{D_o}	drag coefficient at zero angle of attack
C_l	rolling-moment coefficient, $\frac{\text{rolling moment}}{qSb}$
C_{l_β}	$\frac{\partial C_l}{\partial \beta}$
C_L	lift coefficient, $\frac{L}{qS}$
C_{L_α}	$\frac{\partial C_L}{\partial \alpha}$
C_m	pitching-moment coefficient, $\frac{\text{pitching moment}}{qS\bar{c}}$
C_{m_α}	$\frac{\partial C_m}{\partial \alpha}$
C_n	yawing-moment coefficient, $\frac{\text{yawing moment}}{qSb}$
C_{n_β}	$\frac{\partial C_n}{\partial \beta}$
C_N	normal-force coefficient, $\frac{\text{normal force}}{qS}$
C_{N_i}	coefficient of incremental normal force due to interference pressure
C_Y	side-force coefficient, $\frac{\text{side force}}{qS}$
C_{Y_β}	$\frac{\partial C_Y}{\partial \beta}$
D	drag force
l	length of model
L	lift force

M	Mach number
p_b	base pressure
p_∞	free-stream static pressure
q	free-stream dynamic pressure
R_l	free-stream length Reynolds number, $\frac{U}{\nu} l$
S	reference area of wing, $\frac{1}{2} b l$
T_r	recovery temperature
T_w	temperature at model surface
$\frac{U}{\nu}$	Reynolds number per unit length
x_{cp}	axial distance to center of pressure from model apex
α	angle of attack
β	angle of sideslip
Γ	dihedral angle
θ	angle of pitch (wind-tunnel reference system)
Λ	leading-edge sweepback angle
φ	angle of roll (wind-tunnel reference system)

A 3 2 8

DESIGN CONSIDERATIONS

The Original Configuration

The original configuration of reference 1 is sketched in figure 1. It consists of three triangular (half-delta) wing panels symmetrically disposed about an ogive-cylinder body of revolution. The wing root chord is equal to the body length. In the cruising attitude one wing panel lies in a vertical plane and acts as a dorsal fin, while the other two panels serve as the lifting surfaces. The wing anhedral is thus 30°. This symmetrical arrangement was chosen as a means of incorporating favorable static lateral and directional stability (low C_{l_β}, high C_{n_β}). The theoretical advantage of such a symmetrical configuration to minimize C_{l_β} was demonstrated by the analysis of Maple and Synge in reference 5.

The Present Configuration

For the present study, three major modifications were made to the configuration of reference 1 in anticipation of higher lift-drag ratio. First, the anhedral was reduced from 30° to 15°. Theoretically, the lift component of the resultant normal force on each wing panel should increase to a maximum value as the anhedral is reduced to zero. But as the anhedral is reduced, the lateral component of the wing-panel normal force, which helps to provide lateral and directional stability, is also reduced. It was felt that complete elimination of anhedral would adversely affect these stability components. The anhedral of 15° was therefore chosen as an arbitrary compromise.

The second modification consisted of halving the area of the dorsal fin by increasing its leading-edge sweep. This was done to keep the rolling-moment contribution of the dorsal fin (in sideslip) in balance with that of the wings in order to minimize C_{l_β}. Reductions in heat input, friction drag, wave drag, and weight were also realized as a consequence of this modification. Determination of the area to be retained in the dorsal fin was based on the assumption that the side-force contribution of each wing panel was equivalent to that of a ventral fin having an area and shape equal to the projection of the wing panel in a vertical plane.

The third modification consisted of reshaping and relocating the body in an attempt to increase the lift-producing pressure interference on the lower surfaces of the configuration in accordance with the principles outlined in references 6 and 7. For this purpose, the body was modified and placed entirely below the wing. The forward portion of the body consisted of a segment of a blunted circular cone of 12° semiapex angle which extended to 45 percent of the total length. The axis of the cone was tilted upward 2°. At the test Mach number, the cone bow wave was approximately coincident with the wing leading edge (at $\alpha = 0°$) and the cone pressure field covered 30 percent of the total plan-form area. Aft of this conical segment the body was faired toward the wing surfaces to form a flat-bottomed enclosure with a triangular base. Generous fillets were applied to the wing-fin and wing-body junctures to decrease the probability of boundary-layer transition at the wing roots and to reduce the wetted surface area somewhat, while at the same time providing greater structural rigidity and volume. Figure 2 is a sketch of this modified configuration. One final alteration, not associated with the configuration design, became necessary on the test model. Because of strength and flexural limitations of the model support, its shroud could not be made small enough to lie within the design base area of the model. To shield the shroud opening, a fore-and-aft tunnellike fairing was added to the lower aftersurface of the model. The outline of this fairing may be seen in figure 2. Incremental friction and wave drag due to the fairing were considered negligible. The additional base area was included in the calculation of base drag.

As a result of the modifications, the rotational and reflectional symmetry of the original configuration has been reduced in the modified configuration to the conventional single-plane reflectional symmetry. In view of the significant gains in estimated performance which accompany this departure from symmetry, it was considered important in the present experiment to determine whether any reductions in static lateral stability would occur which could be attributed to the reduced symmetry.

Performance Estimates

Estimates of the performance of the original and of the modified configurations were made for the conditions of the present test in order to determine the improvement in aerodynamic performance to be expected from the modifications. The configuration of reference 4, for which experimental data are available, is closely similar to that of reference 1. For comparative purposes, therefore, calculations of minimum drag were also made for the configuration of reference 4. The values of pertinent geometric parameters of these three configurations may be conveniently compared in table I. The principal differences between the configuration of reference 1 and that of reference 4 are that the latter is somewhat shorter and has a considerably blunter wing leading edge.

Minimum-drag coefficients were estimated by summing up the component drag coefficients calculated by methods similar to those used in reference 1. The calculations were made for a Mach number of 3.3, a Reynolds number, R_l, of 5.46×10^6, and a surface temperature equal to recovery temperature. In figure 3 the estimated component drag coefficients of the three configurations are compared. Friction drag is shown for both fully laminar and fully turbulent boundary-layer flow. It is evident that the relatively high drag estimated for the reference 4 configuration is due to the high wave drag of the blunt wing leading edges. The differences in friction drag and base drag between the original (ref. 1) and present configurations are small, as is the difference in total drag. What the present configuration gains in reduced wave drag of the wing it loses in increased wave drag of the lower fineness-ratio body. Part of this increased wave drag is attributed to the fact that the body, considered alone, is at a finite angle of attack. The measured values of minimum total drag from the present test and from reference 4[1] are indicated on figure 3 by the arrows. If the estimated total drag coefficients are assumed to be correct, transition Reynolds numbers of roughly 1 million and 2 million are inferred for the present test and reference 4, respectively.

---

[1]Since foredrag only was reported in reference 4, the plotted value of total drag includes the estimated base drag, and is the interpolated value for a Mach number of 3.30.

Performance at angle of attack was estimated by use of the following equations:

$$C_L = \frac{4}{\sqrt{M^2 - 1}} \alpha \cos^2\Gamma + C_{N_i} - C_{D_o}\alpha \qquad (1)$$

$$C_D = C_{D_o} + \frac{4}{\sqrt{M^2 - 1}} \alpha^2 \cos^2\Gamma + C_{N_i}\alpha \qquad (2)$$

which are based on linear theory and modified to account for wing dihedral and interference normal force. To account for dihedral, the wing panels were assumed to operate as independent flat plates. The angle of attack of each panel is then equal to $\alpha \cos \Gamma$ and the lift component is proportional to $\cos \Gamma$. Interference pressure on the wing due to the body was considered to be effective over the area bounded by the wing leading edge (cone bow wave), the body, and the first ray of the expansion at the end of the conical portion of the body. Over this area the average interference pressure was taken to be the average of the pressure behind the wave and that on the conical surface of the body. Over the remaining portions of the wing and body the interference pressure was assumed to be zero. The interference normal force C_{N_i} was calculated by applying an area-weighted average pressure to the projected area of the effective wing-body surface. The value was calculated for zero angle of attack and was assumed to be independent of α.

In figure 4 is shown the estimated performance of the original configuration (ref. 1) together with the effects of successive modifications. The estimates are made for a Mach number of 3.3, a length Reynolds number, R_l, of 5.46×10^6, and a surface temperature equal to recovery temperature. A transition Reynolds number of 1 million was assumed, and the base pressure coefficient was assumed to be zero (i.e., no base drag). The unmodified configuration has a maximum lift-drag ratio of 4.95 at a lift coefficient of 0.095 and an angle of attack of 5.8°. Reducing the wing anhedral to 15° increases the initial lift-curve slope by about 24 percent and increases the lift-drag ratio to 5.55. This is about 73 percent of the increase in maximum lift-drag ratio which could be achieved by reducing the anhedral to zero. When the leading-edge sweep of the dorsal fin is increased to remove about half of the fin area, the drag coefficient is reduced and the maximum lift-drag ratio is increased to 5.85. Finally, a reshaping of the body to produce favorable interference pressure on the wing panels, while increasing the drag coefficient somewhat, results in a proportionately greater increment in lift coefficient and raises the maximum lift-drag ratio to 6.3. The corresponding lift coefficient is 0.105 and the angle of attack is 3.9°. The modifications, therefore, result theoretically in a 27-percent increase in maximum

lift-drag ratio over that of the unmodified configuration, together with a slight increase in optimum lift coefficient and a significant decrease in optimum angle of attack. At lift coefficients higher than the optimum, the estimated gain in lift-drag ratio increases percentagewise. For example, at a lift coefficient of 0.20 the estimated lift-drag ratio after modification is 5.05, representing a 31-percent gain over the corresponding lift-drag ratio of the original configuration.

EXPERIMENT

The Test Model

The wing panels and dorsal fin of the model were machined separately of steel and then fastened with screws to a center section. The body and fillets were of plastic and were cast directly against the assembled steel parts. A small amount of hand fairing was required at the apex and at the line along which the plastic fillet feathered into the steel wing. The pores of the plastic and the screw holes were filled with hard wax and the model surfaces rubbed fair; however, because of the relatively high turbulence level of the wind tunnel, no attempt was made to produce a surface finish of the quality necessary to ensure that roughness would not affect boundary-layer transition. Photographs of the test model are shown in figure 5.

Wind Tunnel and Instrumentation

The experimental work was conducted in the Ames 1- by 3-Foot Supersonic Wind Tunnel Number 2. This wind tunnel is of the intermittent nonreturn type having flexible nozzle plates which permit operation at any one of several preselected Mach numbers between 1.5 and 3.3. Aerodynamic forces and moments were measured by means of two-, three-, and five-component strain-gage balances. Static pressures at the base of the model were measured with a manometer filled with a low-density oil. During the tests the model and flow field were observed and photographed by means of a schlieren system. Two representative photographs are shown in figure 6.

Test Conditions and Measurements

The Mach number of the air stream at the model location was 3.30 ±0.02. Reynolds number in the free stream was 5.46 million, based on the model length. The model surface temperature was that of an insulated surface.

Aerodynamic forces and moments acting on the model were measured at combined angles of pitch and roll. For each of five roll angles, nominally 0°, $22\text{-}1/2^\circ$, 45°, $67\text{-}1/2^\circ$, and 90°, the model was pitched at 1° and 2° increments between approximately -12° and $+18^\circ$. To assess the small effects of stream angle and of residual trim due to model imperfections, the model was also tested at nominal roll angles of 180° and 270°.

Data Reduction and Precision

The primary data were measured as functions of θ and φ, the angles of pitch and roll, respectively. These data, in coefficient form, were plotted in families of curves as functions of θ for several values of φ. To obtain the coefficients as functions of α and β, the angles of attack and sideslip, respectively, these angles were first determined at every model orientation, in terms of θ and φ, from the test geometry. The primary data were then cross-plotted independently - first as functions of α at various β, and then as functions of β at various α - giving two families of curves. Throughout the presentation all primary data points appear as filled symbols while all cross-plotted points appear as open symbols. Finally, the fairings of the two curve families were iterated to achieve mutual consistency. It is thus possible to estimate the accuracy of the cross-plotting procedure by observing the departure of the iterated curves from the filled symbols, and the departure of the open symbols from the iterated curves.

The precision of the primary data was estimated on the basis of the sensitivity and repeatability of the gages and read-out equipment, and the degree of uncertainty of the dynamic-pressure measurements. The estimated limits of error in the aerodynamic coefficients are tabulated below:

C_N	± 0.004	C_n	± 0.002
C_m	$\pm .002$	C_l	$\pm .0002$
C_A $(\alpha \sim 0^\circ)$	$\pm .0006$	C_L	$\pm .004$
C_A $(\alpha \sim 12^\circ)$	$\pm .001$	C_D $(\alpha \sim 0^\circ)$	$\pm .0006$
C_Y	$\pm .002$	C_D $(\alpha \sim 12^\circ)$	$\pm .0024$

Angles of pitch and roll were measured within $\pm 0.2^\circ$. Pitch-angle measurements were adjusted to account for a stream angularity of -0.2°.

RESULTS AND DISCUSSION

Primary Data

The primary-force measurements, reduced to coefficient form in the body-axis system, are presented in figure 7, in which the coefficients are plotted versus angle of pitch for a constant angle of roll. With the exception of the coefficient of axial force due to base pressure, C_{A_b}, these data are subsequently cross-plotted. For all the model attitudes tested, the value of C_{A_b} remained approximately constant at 0.004.

Aerodynamic Characteristics at Zero Sideslip

Lift coefficient is plotted versus angle of attack, pitching-moment coefficient, drag coefficient, and lift-drag ratio in figure 8. The angle of sideslip, β, is zero for these data. Curves of lift-drag ratio are shown based both on total drag and on foredrag (total drag minus base drag). The lift coefficient at maximum lift-drag ratio (based on total drag) is 0.125, and the corresponding angle of attack is 4.7°. The pitching-moment coefficient is linear within the range of measurement. The maximum lift-drag ratio of the model in the upright attitude (positive α) is greater than that in the inverted attitude (negative α) by 8 percent when based on total drag, and by 20 percent when based on foredrag. It is significant that at lift coefficients as large as 0.35 (angles of attack up to 15.3°) the lift-drag ratio remains greater than 3.

In figure 9 the measured lift-drag ratio is compared with the estimated L/D of the test model and with experimental results from reference 4. The lift-drag ratios are based on foredrag coefficient. There is a small increase in the predicted L/D plotted here over that shown in figure 4 due to the sharper leading edge of the test model. Interference lift at zero angle of attack, drag, and lift-drag ratio are predicted satisfactorily by equations (1) and (2), while initial lift-curve slope and lift are somewhat underestimated. At a lift coefficient of 0.20 the estimated lift falls about 5 percent below the experimental curve.

Comparison of the present results with those of reference 4 ($\Gamma = -15^\circ$) shows significantly higher lift-drag ratios for the present configuration. The lower zero-lift drag of the present model is due largely to the smaller leading-edge bluntness while the higher lift coefficient at a given α is due largely to favorable pressure interference, although the aspect ratio is significantly greater also. The present model has a higher $\partial C_m/\partial C_L$ than does the configuration of reference 4. It has a positive C_m at $\alpha = 0^\circ$ and therefore requires less trimming moment to fly at lift

coefficients less than 0.2. This result is also attributed to the difference in leading-edge bluntness and to favorable pressure interference on the present configuration.

Aerodynamic Characteristics at Combined Angles

Longitudinal characteristics.- The variations of normal-force coefficient, pitching-moment coefficient, and axial-force coefficient with angle of attack at several constant angles of sideslip are presented in figure 10. The variations of these coefficients with angle of sideslip at several constant angles of attack are shown in figure 11. Within the range of angles covered in the test, the effects of sideslip on the longitudinal characteristics are small. Examination of figures 11(a) and 11(c) indicates that no reduction in L/D should occur for moderate departures of β from zero.

Longitudinal derivatives and center-of-pressure position are presented as functions of sideslip angle in figure 12. The curves were derived from slope measurements of the curves of figures 8 and 10. Figure 12 shows that the initial lift-curve slope ($\alpha = 0^{\circ}$) is virtually invariant with β in the range of measurement. The predicted initial lift-curve slope, obtained by differentiation of equation (1), is smaller than the measured value by approximately 10 percent as shown in the figure. The longitudinal center of pressure remains nearly fixed at combined angles of attack and sideslip when α is zero or positive, and at negative angles of attack when β is zero (fig. 12). At negative angles of attack there is a more pronounced forward shift of the center of pressure with increasing β. When compared to the centroid of area of a triangular wing ($(2/3)l$) and to the positions shown for the configurations of references 3 and 4, the center of pressure of the present configuration lies relatively far aft. This fact contributes to its comparatively high level of longitudinal stability.

Lateral and directional characteristics.- The variations of rolling-moment coefficient, yawing-moment coefficient, and side-force coefficient with angle of sideslip at several constant angles of attack are plotted in figure 13. The variations of these coefficients with angle of attack at several constant angles of sideslip are shown in figure 14. Figures 13(a) and 14(a) indicate that rolling moments remain relatively small and have regular variation within the range of angles of the test. Note that the usual sign convention is used here - positive rolling moment is a clockwise moment when the airplane is viewed from the rear.

The model is directionally stable at all angles and has relatively linear yawing-moment characteristics at positive angles of attack. It is evident in figure 14(b), however, that with increasing negative α these characteristics become significantly nonlinear, possibly as the result of flow separation from the leading edge of the forward wing.

Lateral and directional derivatives and center-of-pressure position are presented as functions of angle of attack in figures 15 and 16. These curves were derived from slope measurements of the curves of figure 13. The lateral stability with respect both to body axes and to stability axes is plotted in figure 15.

With respect to body axes, the model exhibits increasing positive effective dihedral with increasing positive angle of attack, and increasing negative effective dihedral with increasing negative angle of attack. About the stability axis the model exhibits qualitatively the same characteristic for angles of attack greater than about -4°. At more negative angles of attack the effective dihedral decreases until at $\alpha = -9.5^\circ$ it appears to become negative. The fairly small values of C_{l_β} measured for the present model appear to validate the design criterion (discussed previously) used for reducing the area of the dorsal fin to compensate for the reduced anhedral. Small changes in anhedral or fin leading-edge sweep angle should prove an effective means of tailoring the lateral stability characteristics to fit given requirements for configurations of this type.

The directional stability of the model (fig. 16) deteriorates with increasing positive angle of attack and improves with increasing negative angle of attack. This result is in accord with the expected effectiveness of the dorsal fin as the angle of attack is varied. At $\alpha = 12^\circ$, the directional stability is about 60 percent of the value at $\alpha = 0^\circ$. At the cruising angle of attack of 4.7°, C_{n_β} is about 85 percent of the value at $\alpha = 0^\circ$.

The directional center of pressure when sideslip is zero is very close to $(2/3)l$ at $\alpha = 0^\circ$ (fig. 16) and moves slowly forward as α departs from zero. At positive angles of attack, the directional center of pressure remains 3 or 4 percent of l forward of the longitudinal center of pressure.

CONCLUDING REMARKS

Comparison of the experimental results with the estimated performance of the modified configuration indicates that, in general, the expected aerodynamic benefits of the modifications were realized. The experimental maximum lift-drag ratio of 6.65 (excluding base drag) at a lift coefficient of 0.100 and angle of attack of 3.6° is in good agreement with the estimated maximum lift-drag ratio. This lift-drag ratio is 31 percent higher than that estimated for the unmodified configuration. The experimental results further indicate that within the range of angles of the test the static stability characteristics of the modified configuration are favorable. The positions of the longitudinal and lateral centers of

pressure are weakly dependent on attitude and in general remain slightly aft of the respective centroids of projected plan-form and side area. While there are no stability data at supersonic speeds for the original configuration (other than C_{m_α} at $\beta = 0^\circ$ from ref. 4) with which to make a comparison, it seems clear on the basis of the present results that little, if any, deterioration of desirable static stability characteristics has been suffered as a result of the loss of rotational and reflectional symmetry due to the design modifications.

Ames Research Center
National Aeronautics and Space Administration
Moffett Field, Calif., May 6, 1960

REFERENCES

1. Seiff, Alvin, and Allen, H. Julian: Some Aspects of the Design of Hypersonic Boost-Glide Aircraft. NACA RM A55E26, 1955.

2. Delany, Noel K.: Exploratory Investigation of the Low-Speed Static Stability of a Configuration Employing Three Identical Triangular Wing Panels and a Body of Equal Length. NACA RM A55C28, 1955.

3. Delany, Noel K.: Additional Measurements of the Low-Speed Static Stability of a Configuration Employing Three Triangular Wing Panels and a Body of Equal Length. NACA RM A55F02a, 1955.

4. Savin, Raymond C., and Wong, Thomas J.: Lift, Drag, and Static Longitudinal Stability Characteristics of Configurations Consisting of Three Triangular Wing Panels and a Body of Equal Length at Mach Numbers From 3.00 to 6.28. NACA RM A55K21, 1956.

5. Maple, C. G., and Synge, J. L.: Aerodynamic Symmetry of Projectiles. Quart. Appl. Math., vol. VI, no. 4, Jan. 1949, pp. 345-366.

6. Ferri, Antonio, Clarke, Joseph H., and Cassacio, Anthony: Drag Reduction in Lifting Systems by Advantageous Use of Interference. PIBAL Rep. 272, Polytechnic Institute of Brooklyn, Dept. of Aero. Eng. and Appl. Mech., May 1955.

7. Eggers, A. J., Jr., and Syvertson, Clarence A.: Aircraft Configurations Developing High Lift-Drag Ratios at High Supersonic Speeds. NACA RM A55L05, 1956.

TABLE I.- GEOMETRIC PARAMETERS OF THREE SIMILAR CONFIGURATIONS

	Present configuration	Configuration of ref. 1 (see fig. 1)	Configuration of ref. 4
Aspect ratio, two wing panels	1.46	1.16	1.15
Fineness ratio of body	[1]6.8	9.5	7.0
Wing area, two panels	$0.36\ l^2$	$0.29\ l^2$	$0.29\ l^2$
Mean aerodynamic chord	$(2/3)\ l$	$(2/3)\ l$	$(2/3)\ l$
Dihedral angle	-15°	-30°	$-15^\circ, -30^\circ, 0^\circ$
Leading-edge sweep angle of wing	70°	73.85°	74°
Leading-edge sweep angle of fin	79.2°	73.85°	74°
Root thickness ratio of wing	0.024	0.020	0.020
Root thickness ratio of fin	0.014	0.020	0.020
Leading-edge radius of wing and fin	$0.000864\ l$	$0.00132\ l$	$0.00357\ l$
Nose apex radius	$0.00435\ l$	$0.00263\ l$	$0.00357\ l$

[1]Based on an equivalent body diameter: $\sqrt{\frac{4}{\pi} A_{max}}$

Body fineness ratio - 9.5
Nose - tangent ogive of fineness ratio 5, with tip blunted to spherical radius of 5% of maximum body radius
b/d = 5.5
Wing thickness ratio - 2% at root
Cylindrical leading edge of constant radius = .066 maximum wing thickness

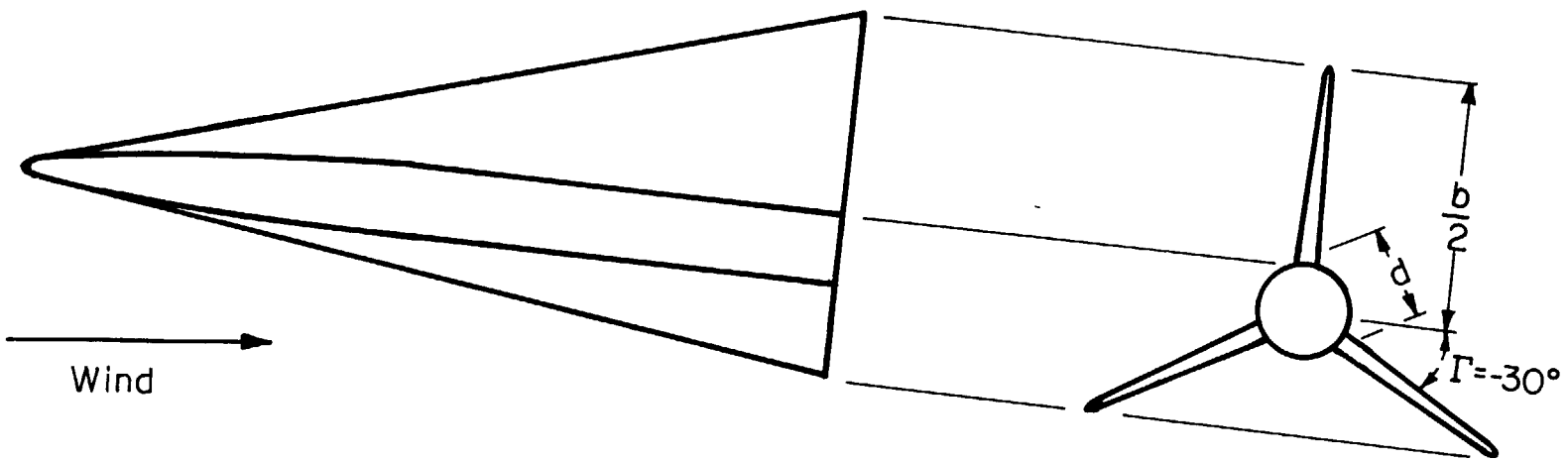

Figure 1.- Configuration of reference 1.

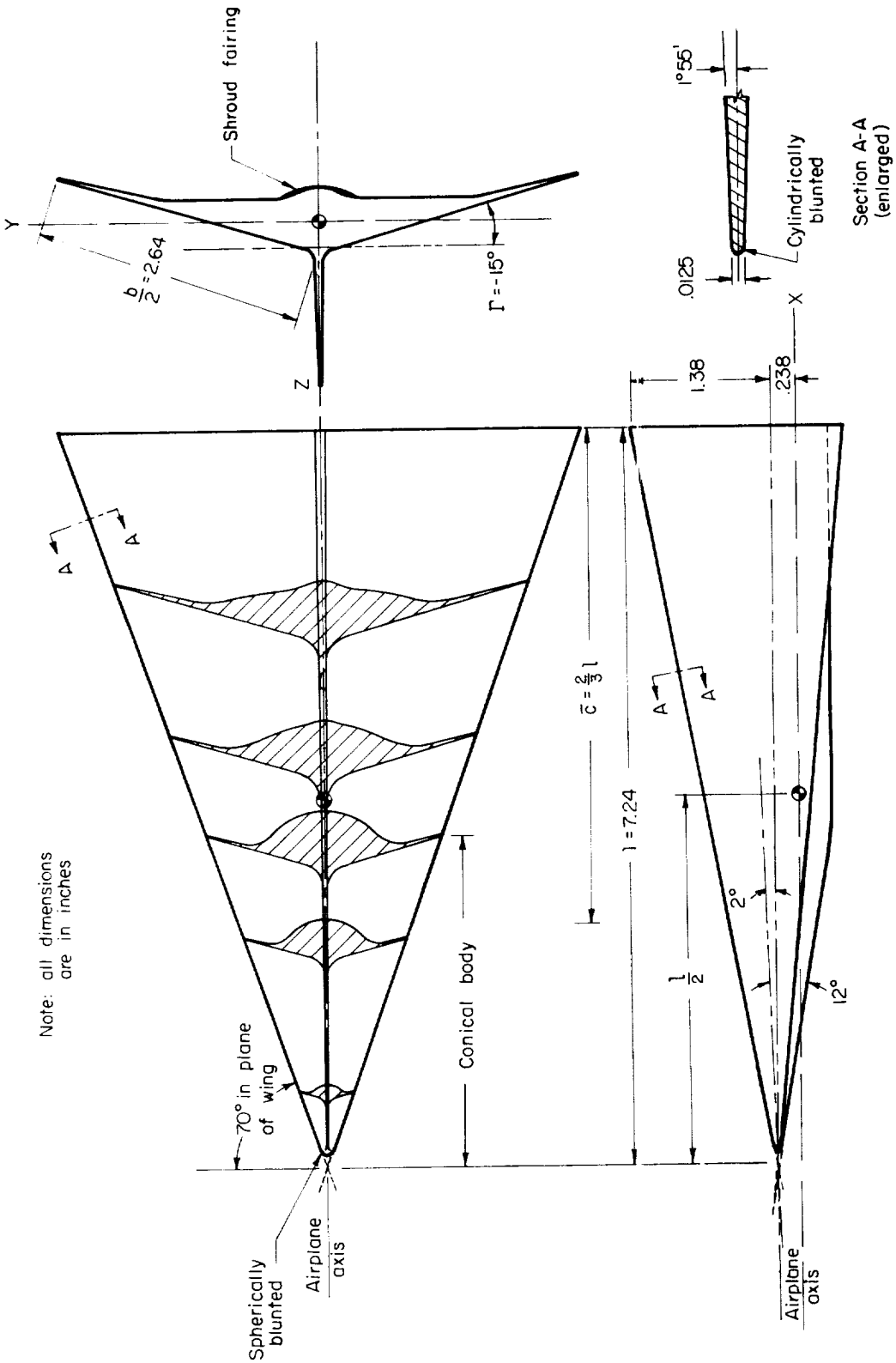

Figure 2.- Sketch of the test configuration.

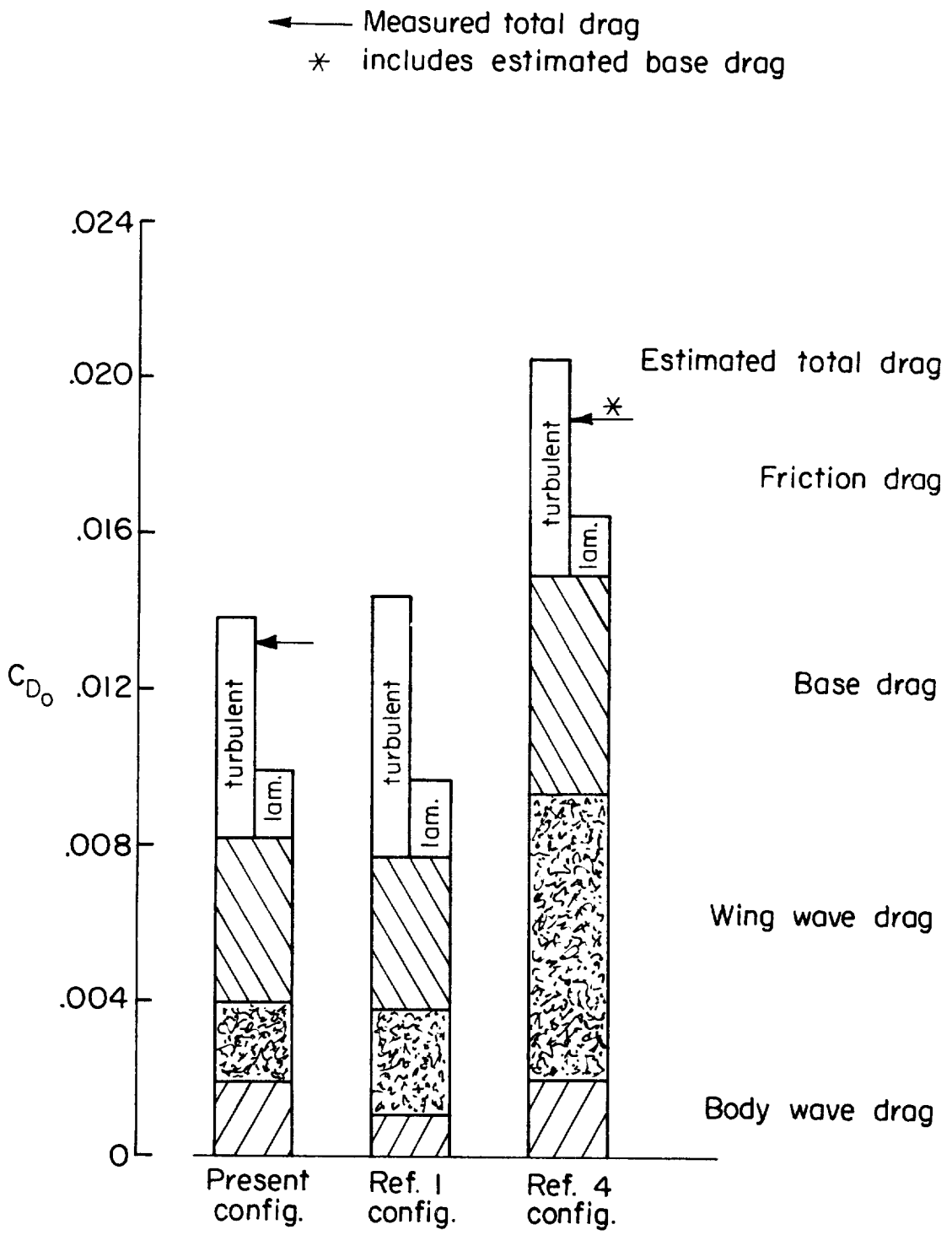

Figure 3.- Estimated drag coefficients at zero angle of attack; M = 3.30, $R_l = 5.46 \times 10^6$, $T_w = T_r$.

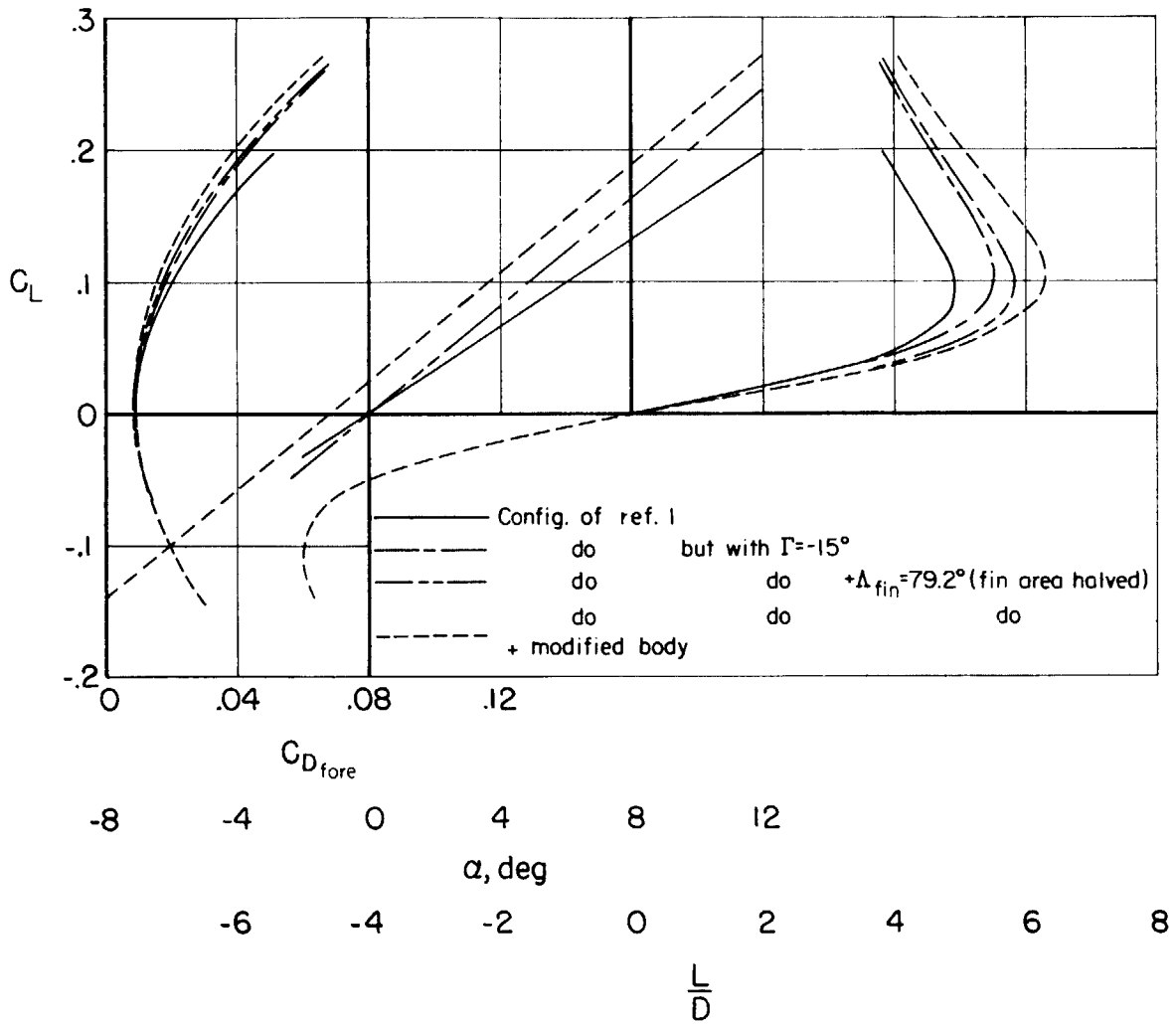

Figure 4.- Estimated effects of geometric modifications on the lift and drag characteristics at $M = 3.30$, $R_l = 5.46 \times 10^6$, $T_w = T_r$.

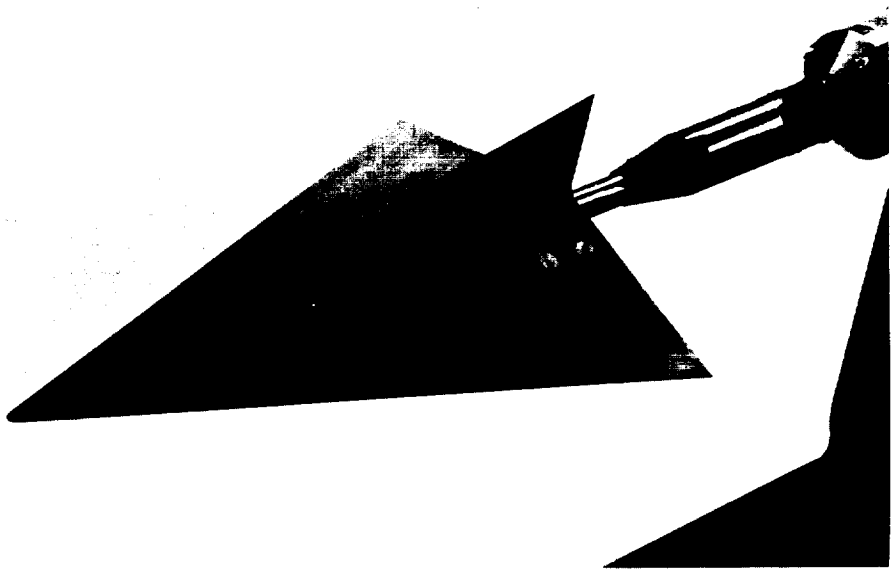

A-22520

(a) View from above.

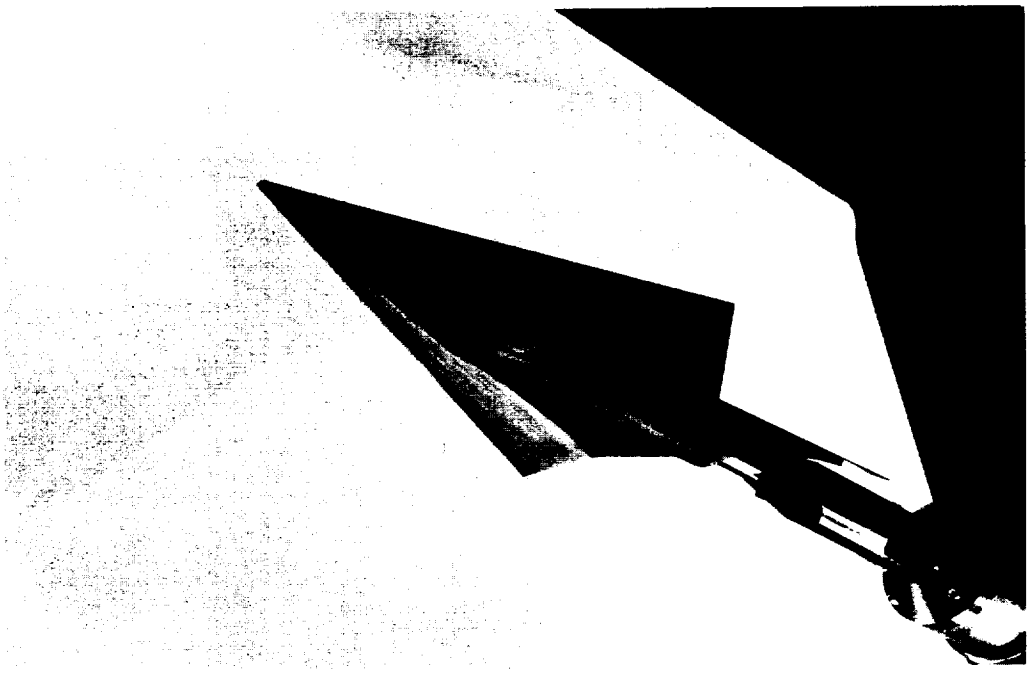

A-22521

(b) View from below.

Figure 5.- Photographs of test model.

$\alpha = 0^{\circ}$

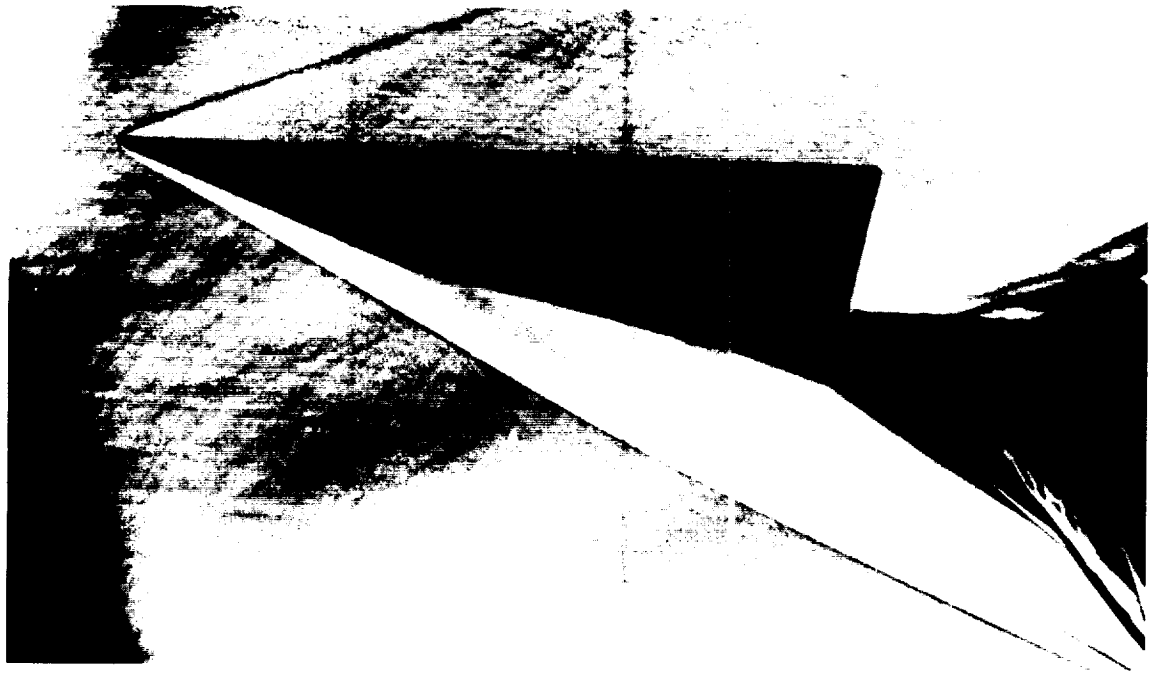

$\alpha = 12.5^{\circ}$

Figure 6.- Schlieren photographs of the test model; $\beta = 0^{\circ}$.

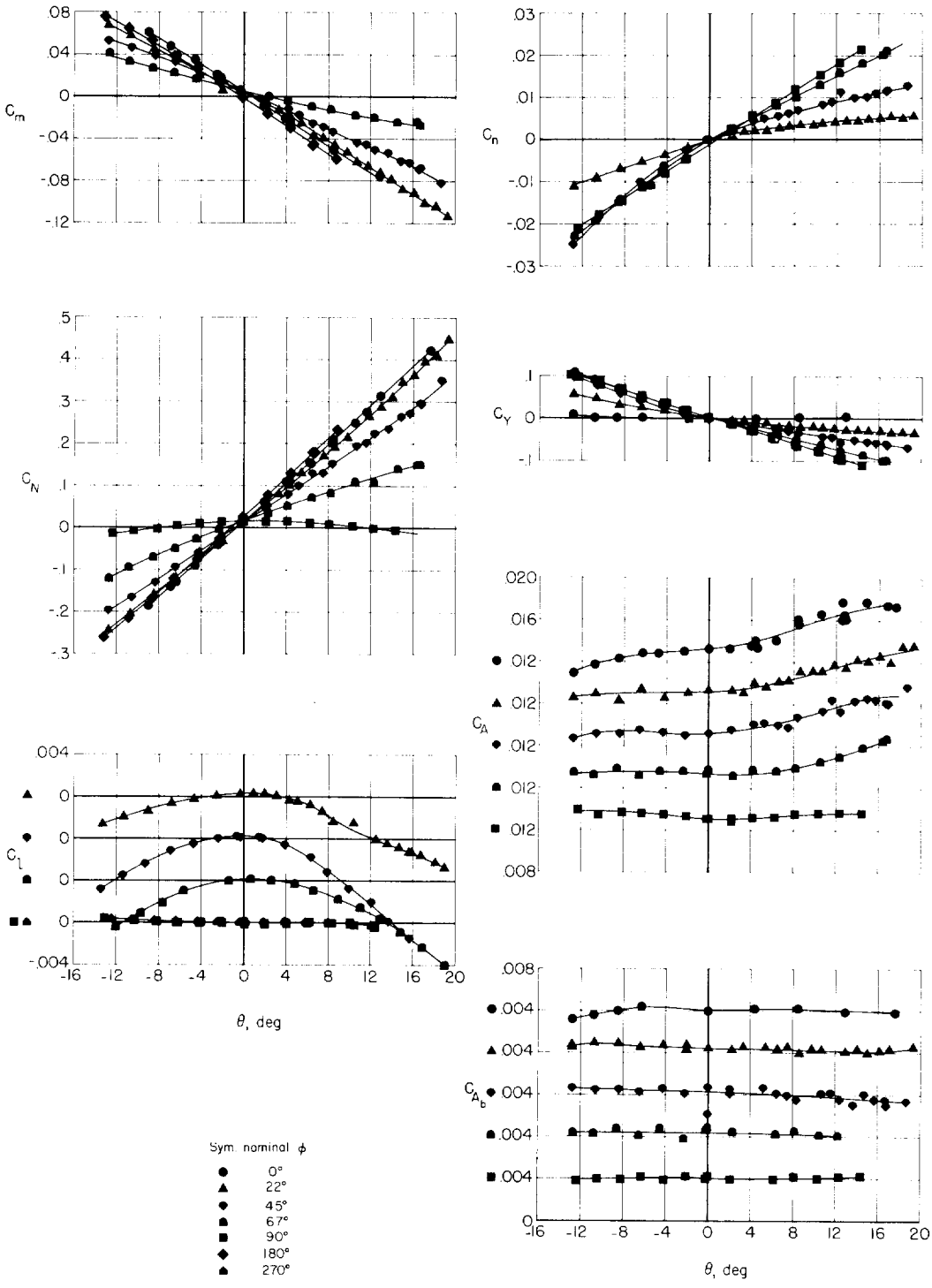

Figure 7.- Static aerodynamic characteristics in combined pitch and roll.

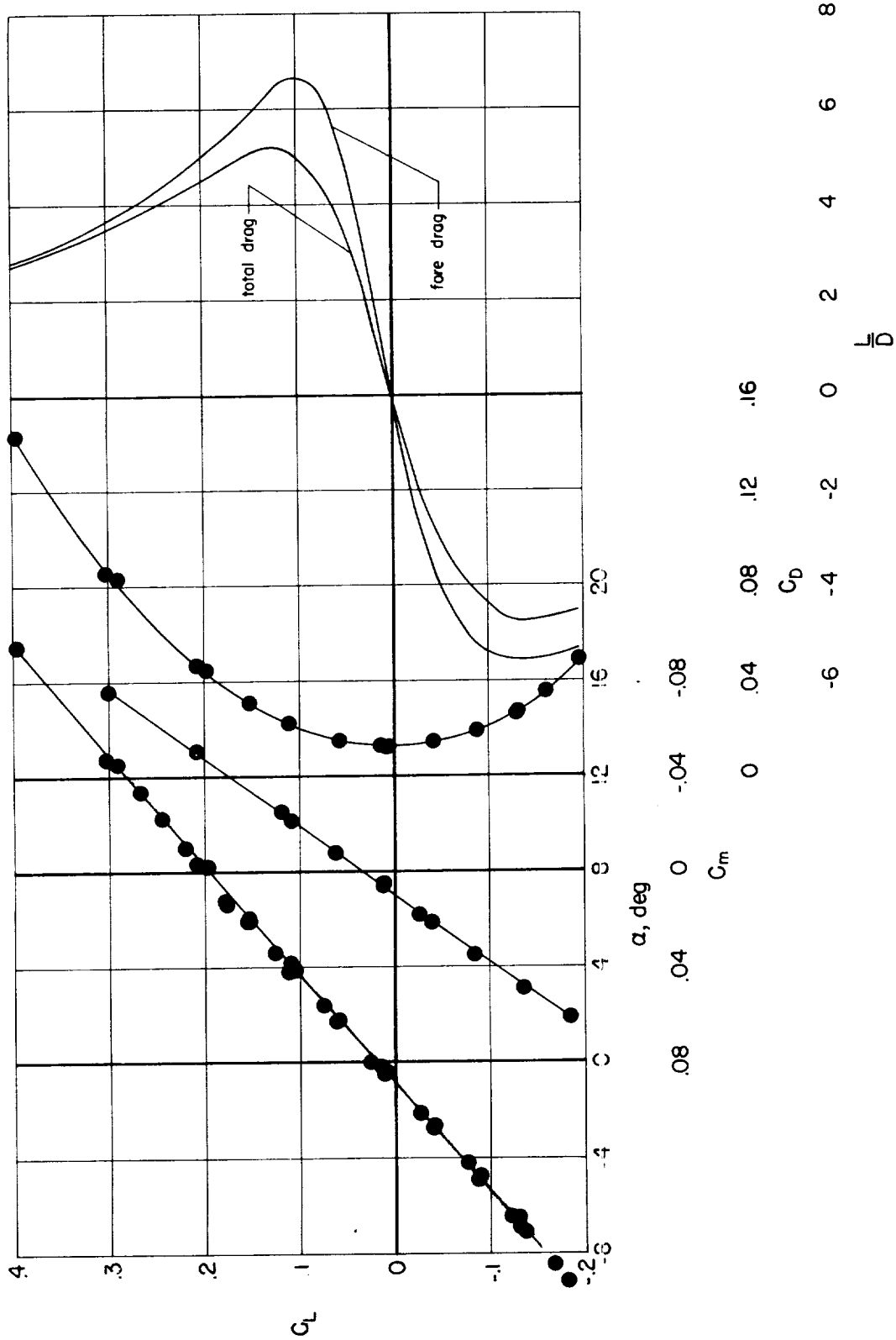

Figure 8.- Longitudinal characteristics; $\beta = 0^{\circ}$.

A
∞ 2 ω

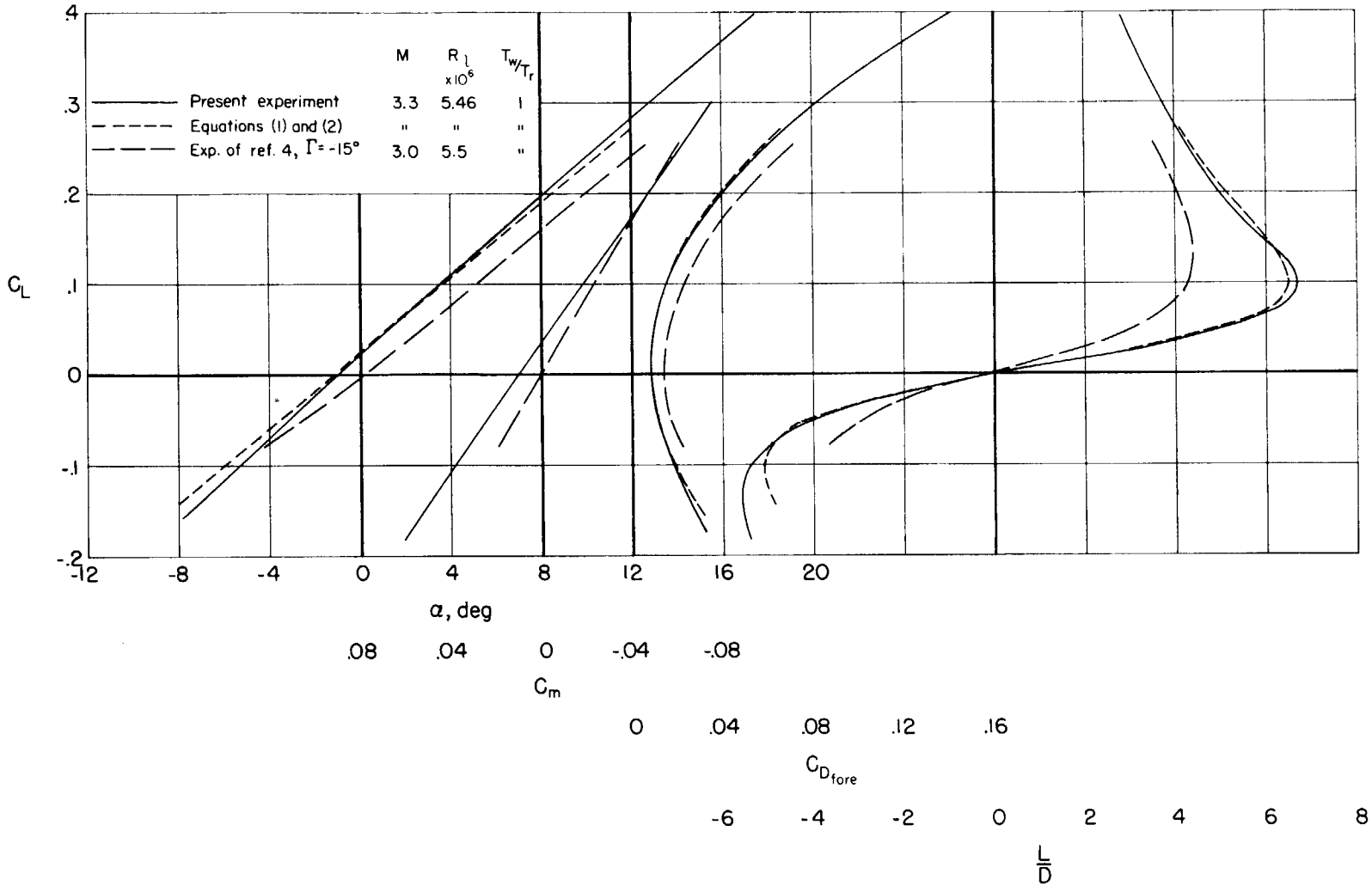

Figure 9.- Comparison of measured and estimated longitudinal characteristics; $\beta = 0^{\circ}$.

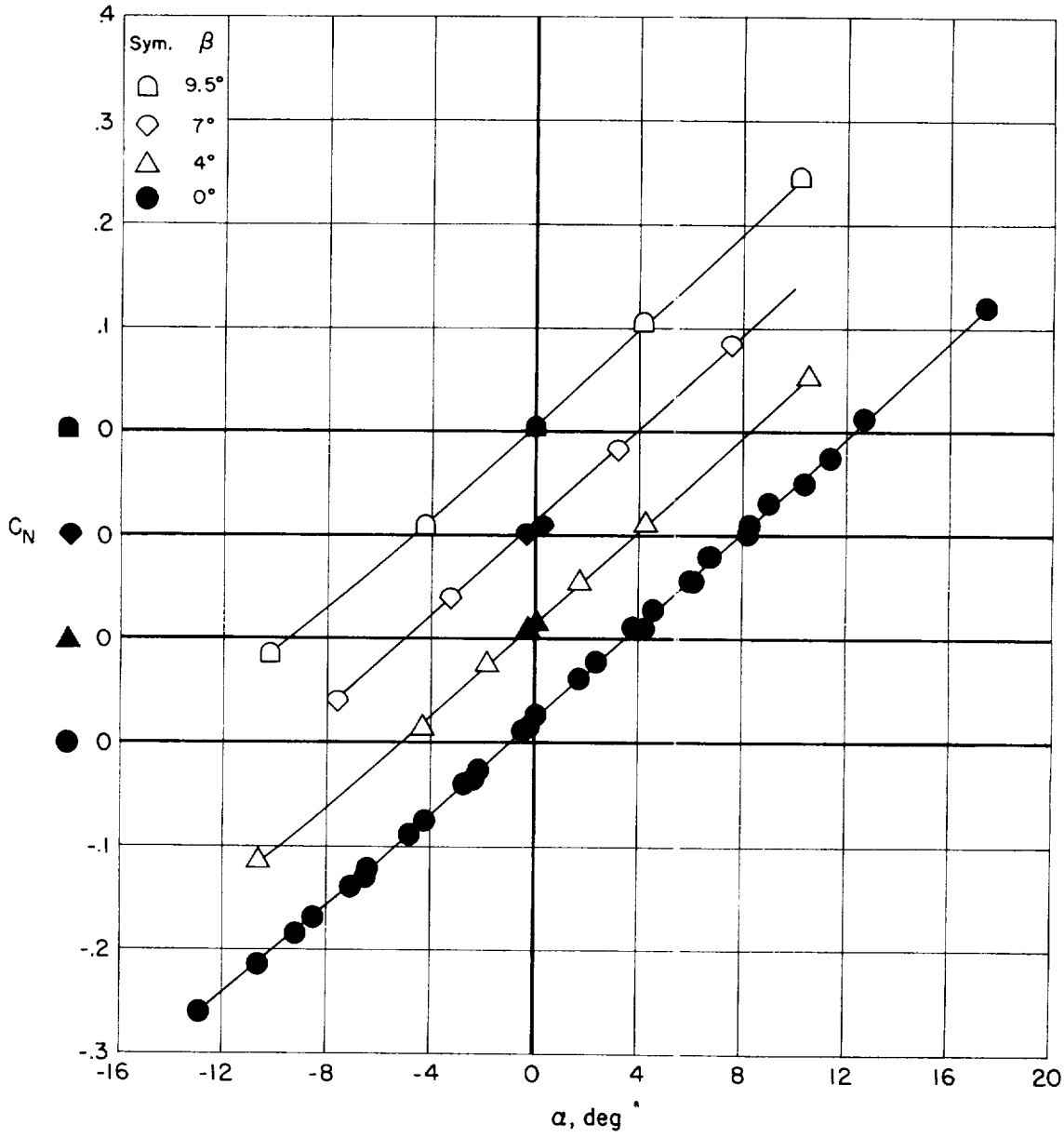

(a) Normal-force coefficient.

Figure 10.- Variations of static longitudinal characteristics with angle of attack at several angles of sideslip.

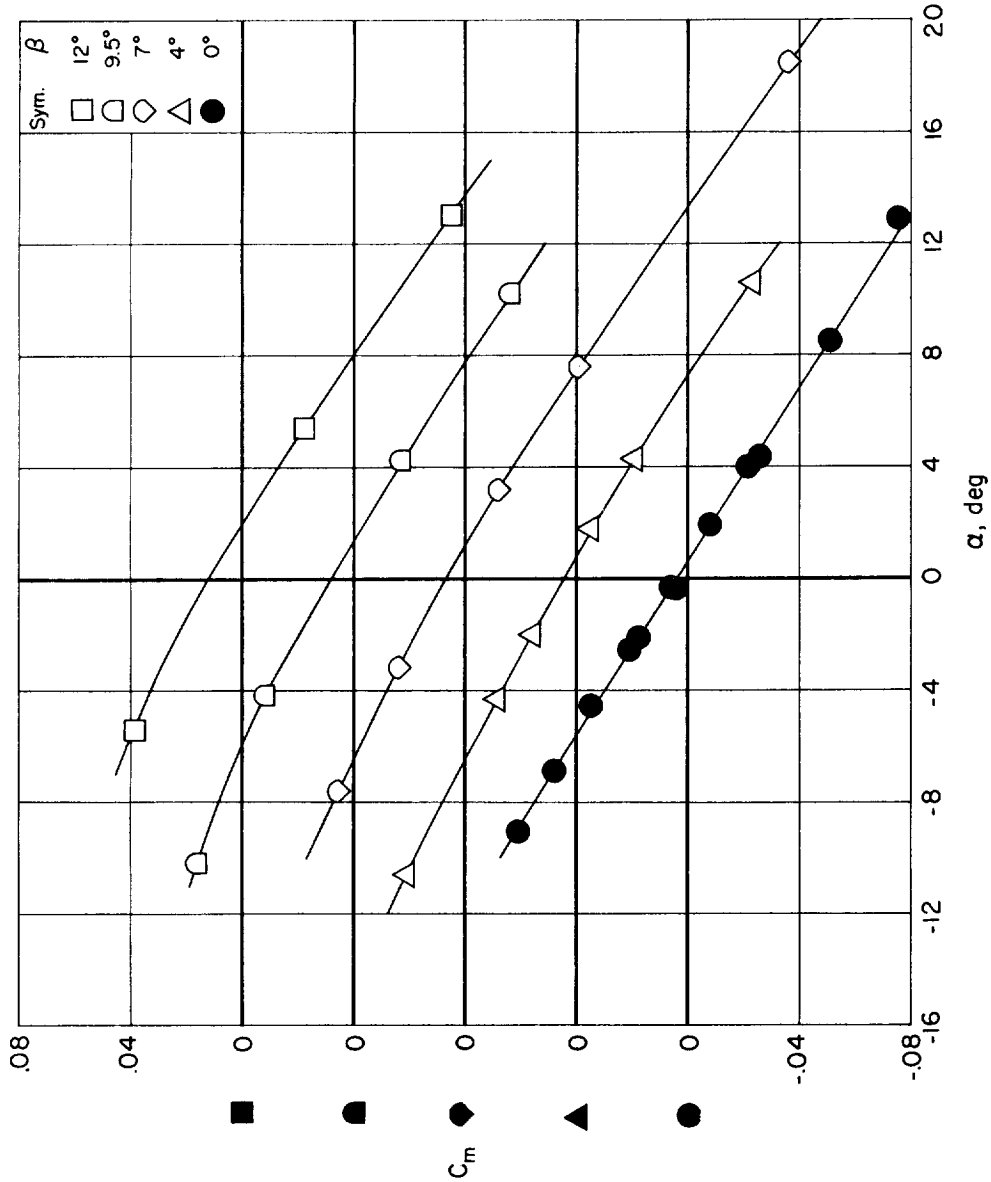

(b) Pitching-moment coefficient.

Figure 10.- Continued.

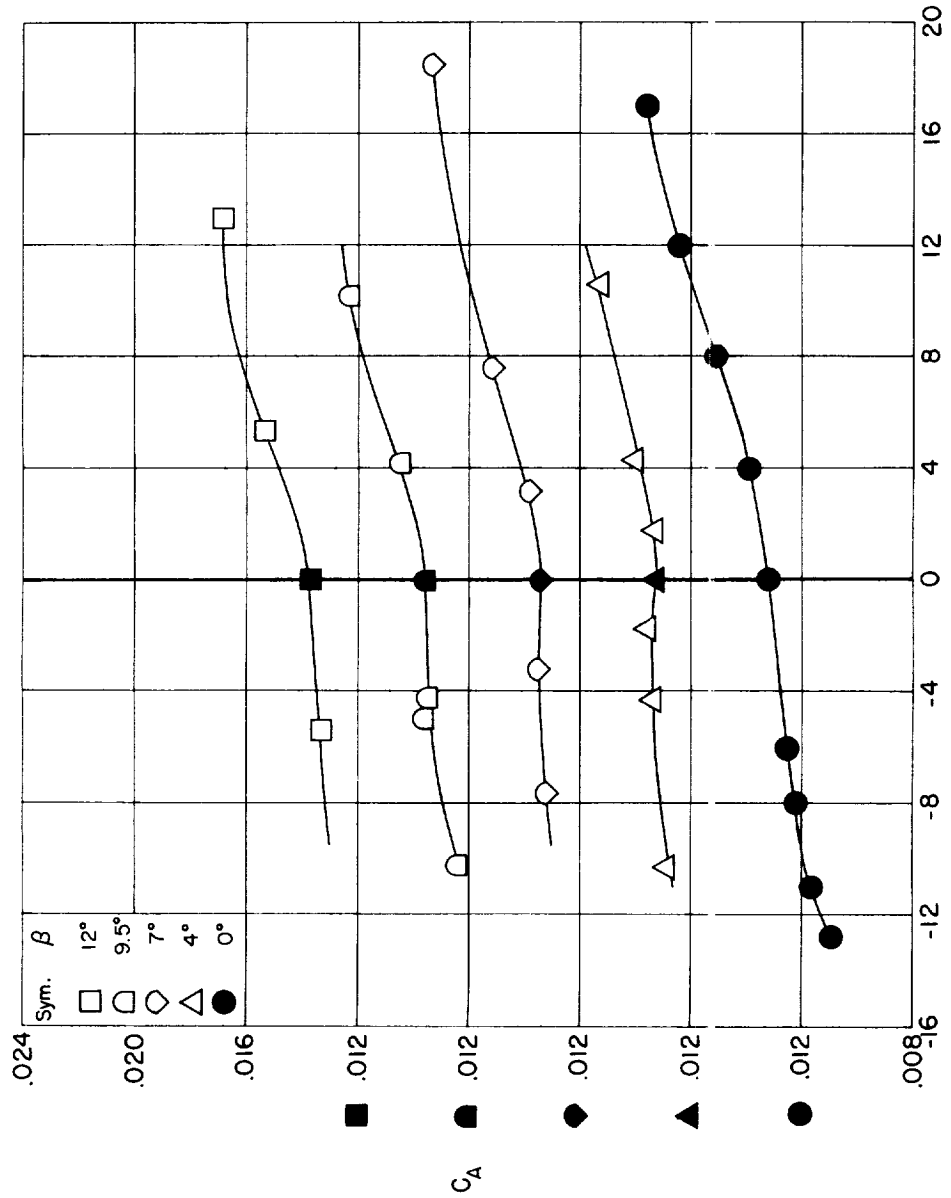

(c) Axial-force coefficient.

Figure 10.- Concluded.

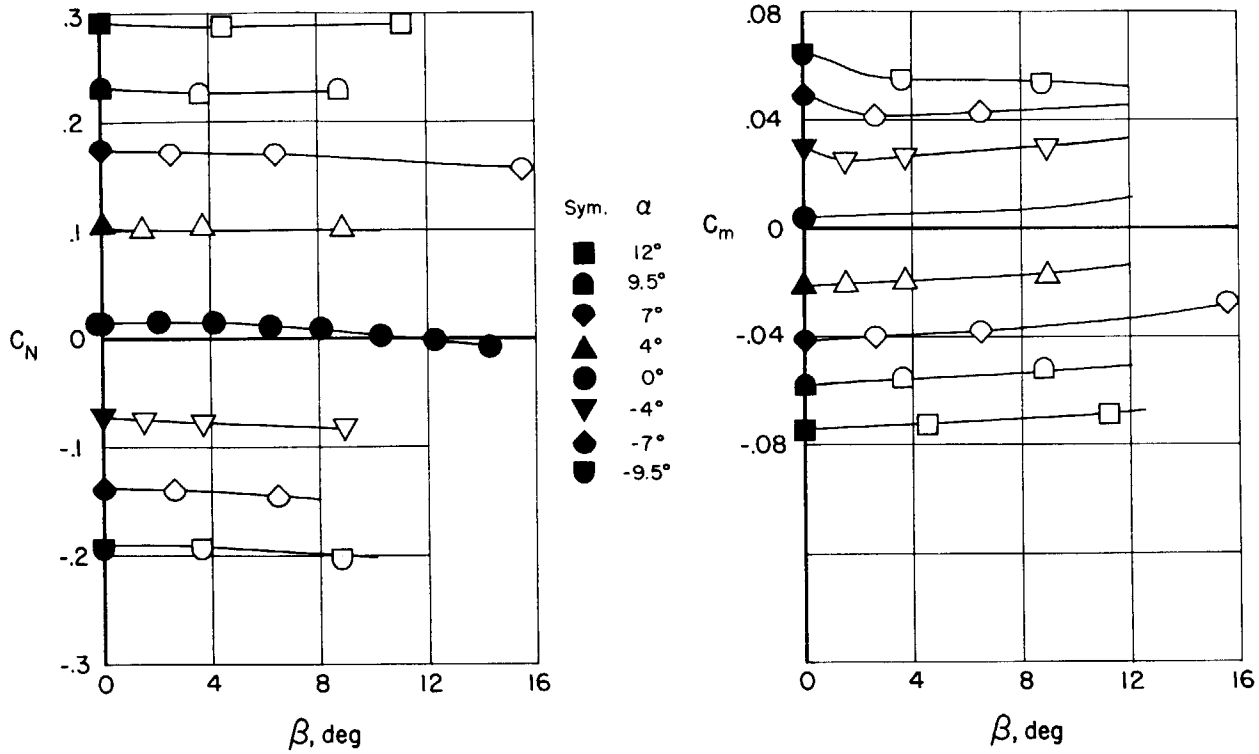

(a) Normal-force coefficient.

(b) Pitching-moment coefficient.

Figure 11.- Variations of static longitudinal characteristics with angle of sideslip at several angles of attack.

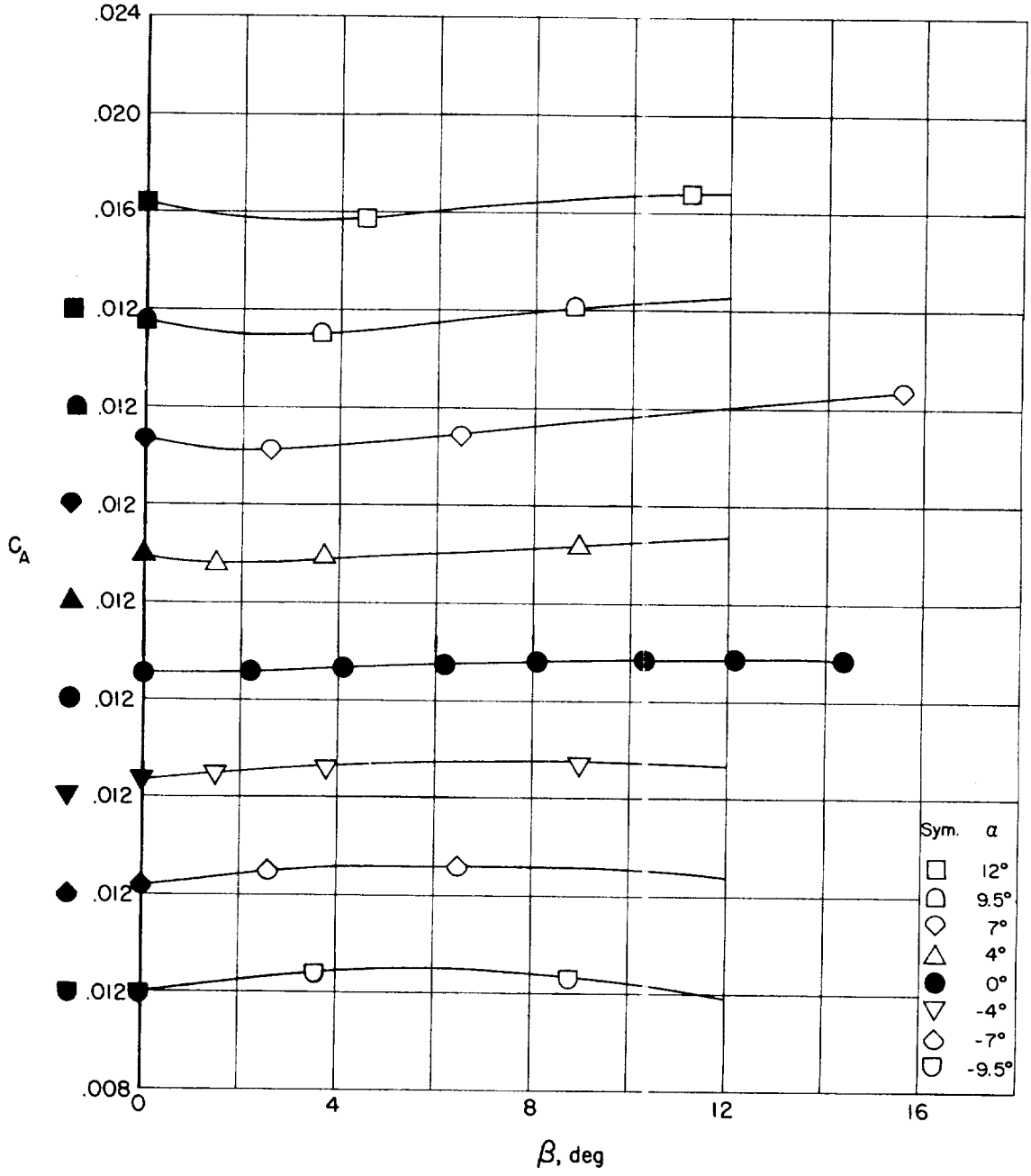

(c) Axial-force coefficient.

Figure 11.- Concluded.

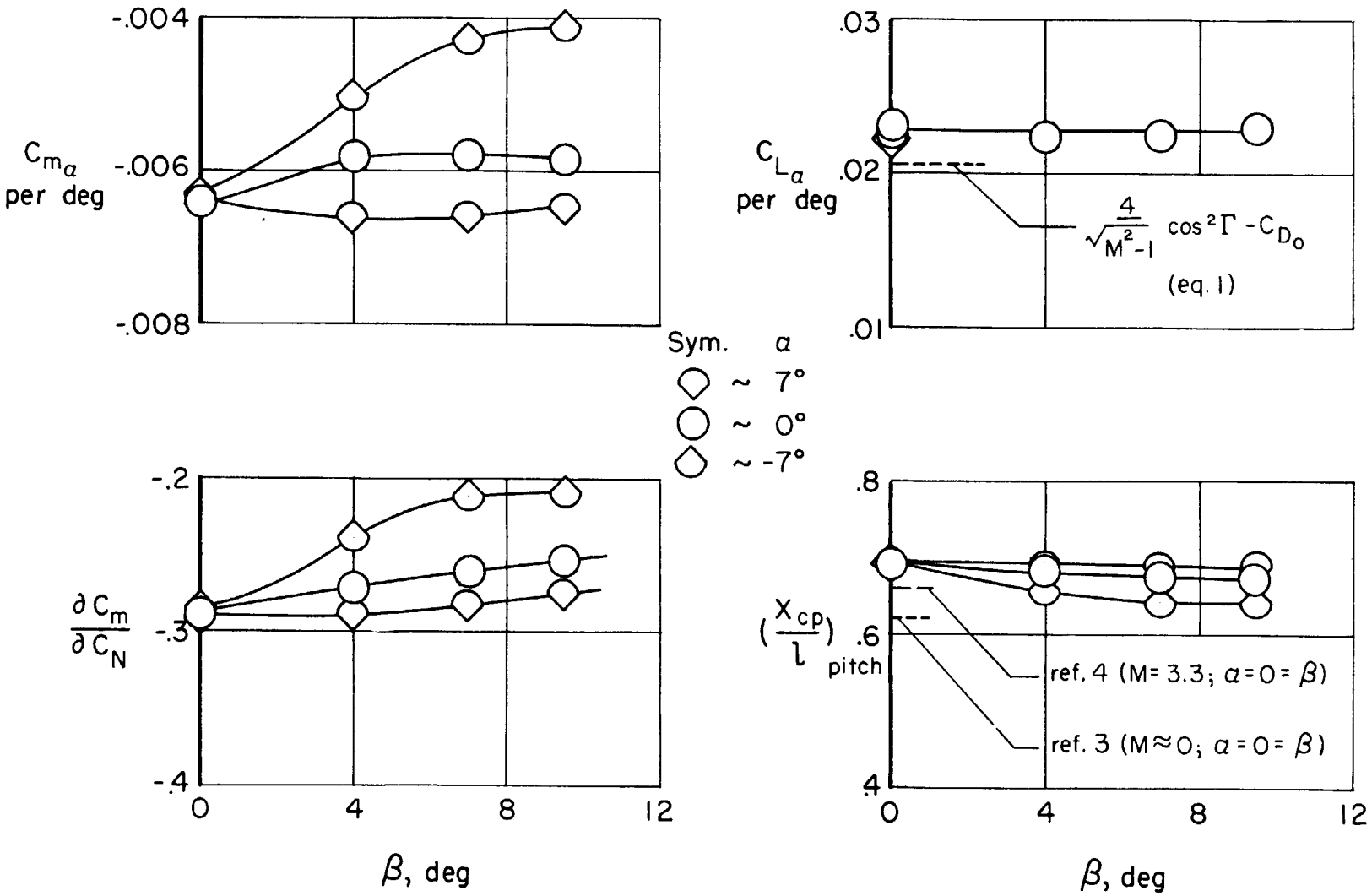

Figure 12.- Variations of longitudinal derivatives and center-of-pressure position with angle of sideslip at three angles of attack.

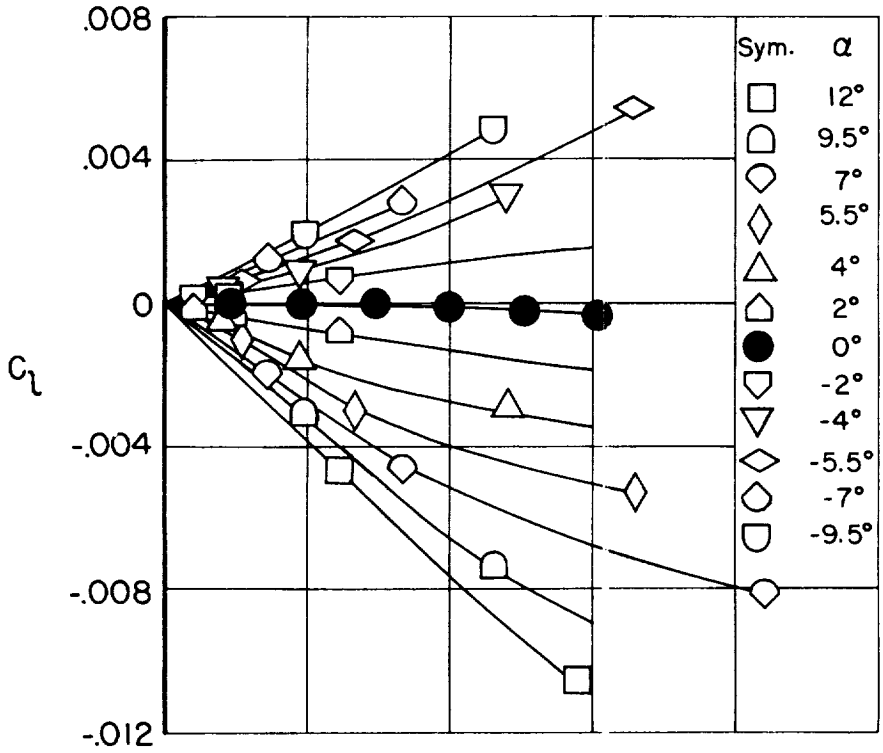

(a) Rolling-moment coefficient.

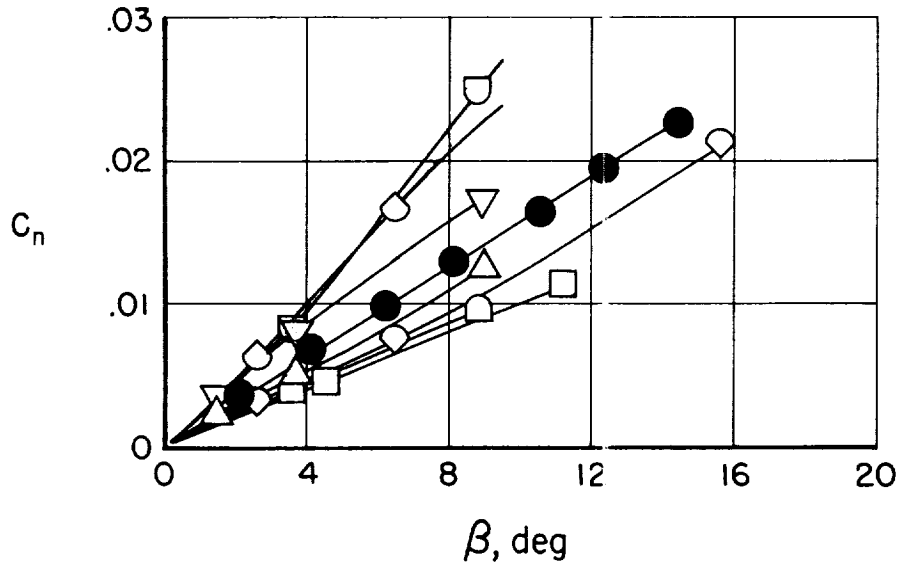

(b) Yawing-moment coefficient.

Figure 13.- Variations of static lateral and directional charcteristics with angle of sideslip at several angles of attack.

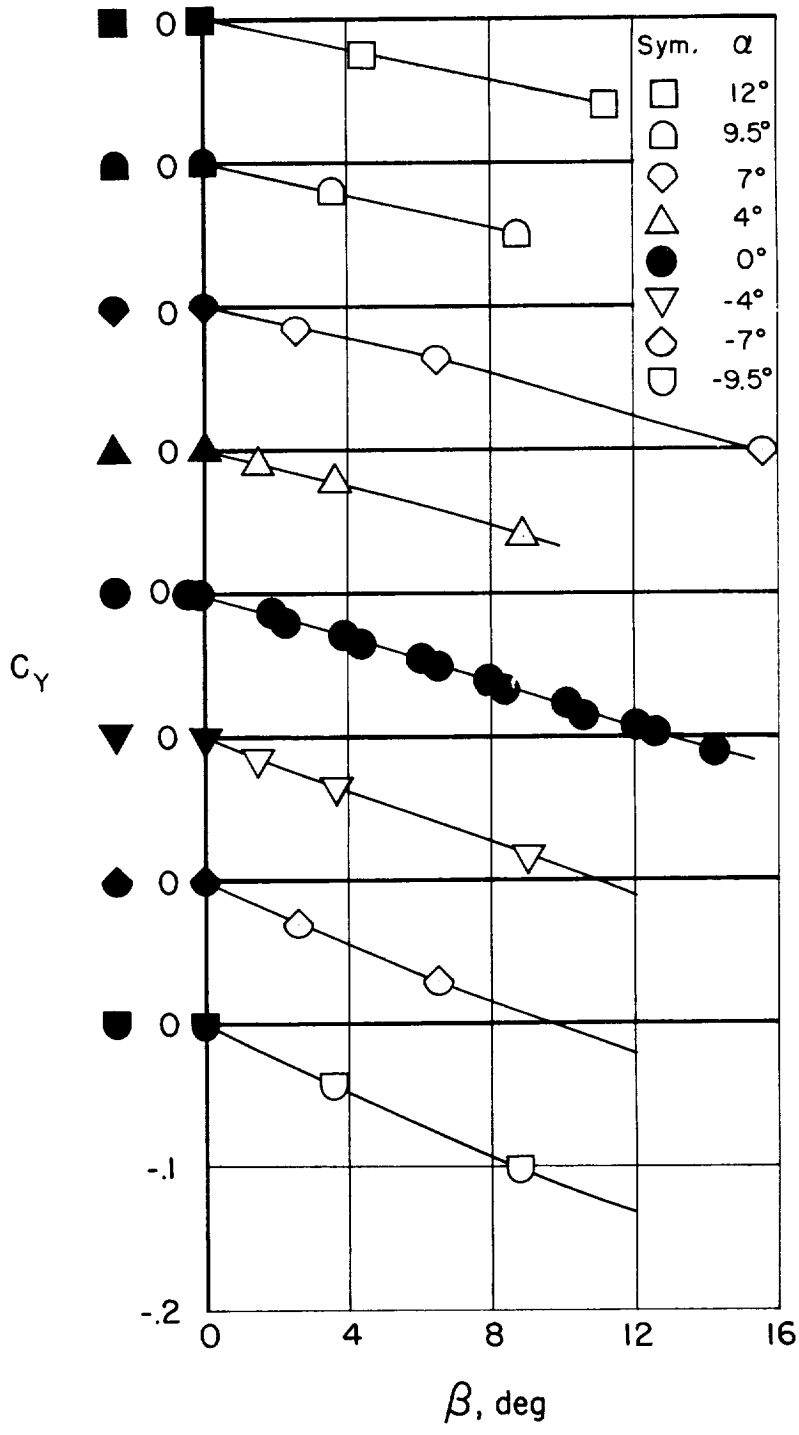

(c) Side-force coefficient.

Figure 13.- Concluded.

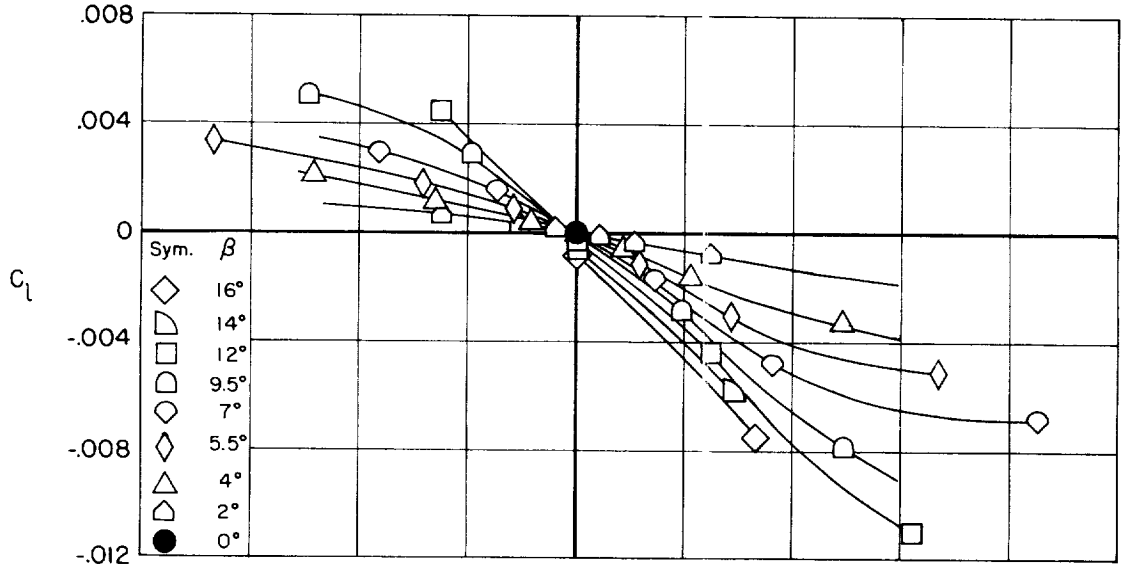

(a) Rolling-moment coefficient.

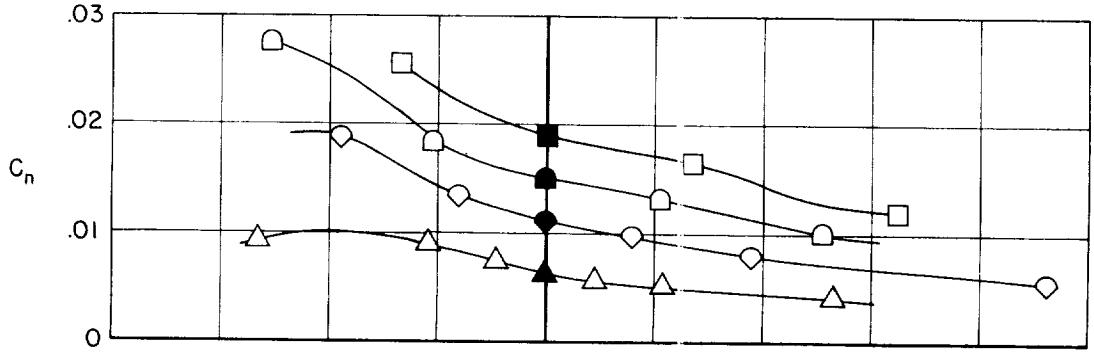

(b) Yawing-moment coefficient.

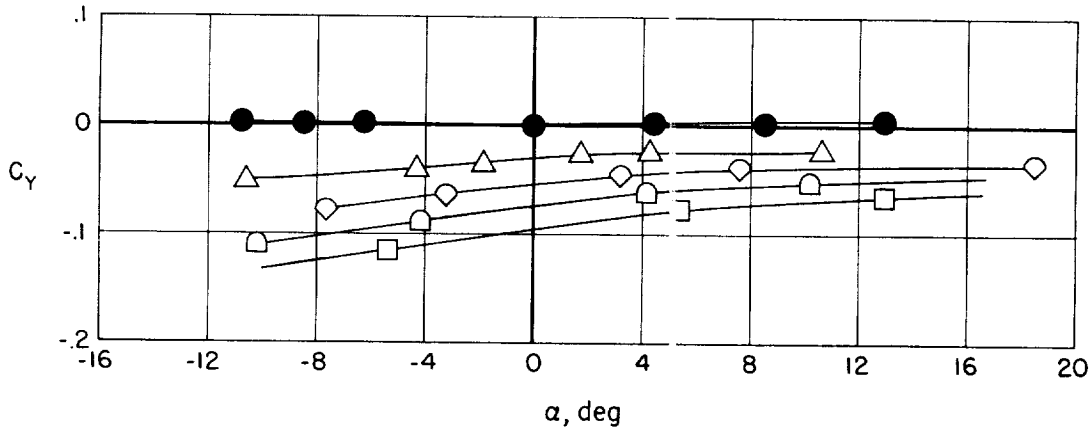

(c) Side-force coefficient.

Figure 14.- Variations of static lateral and directional characteristics with angle of attack at several angles of sideslip.

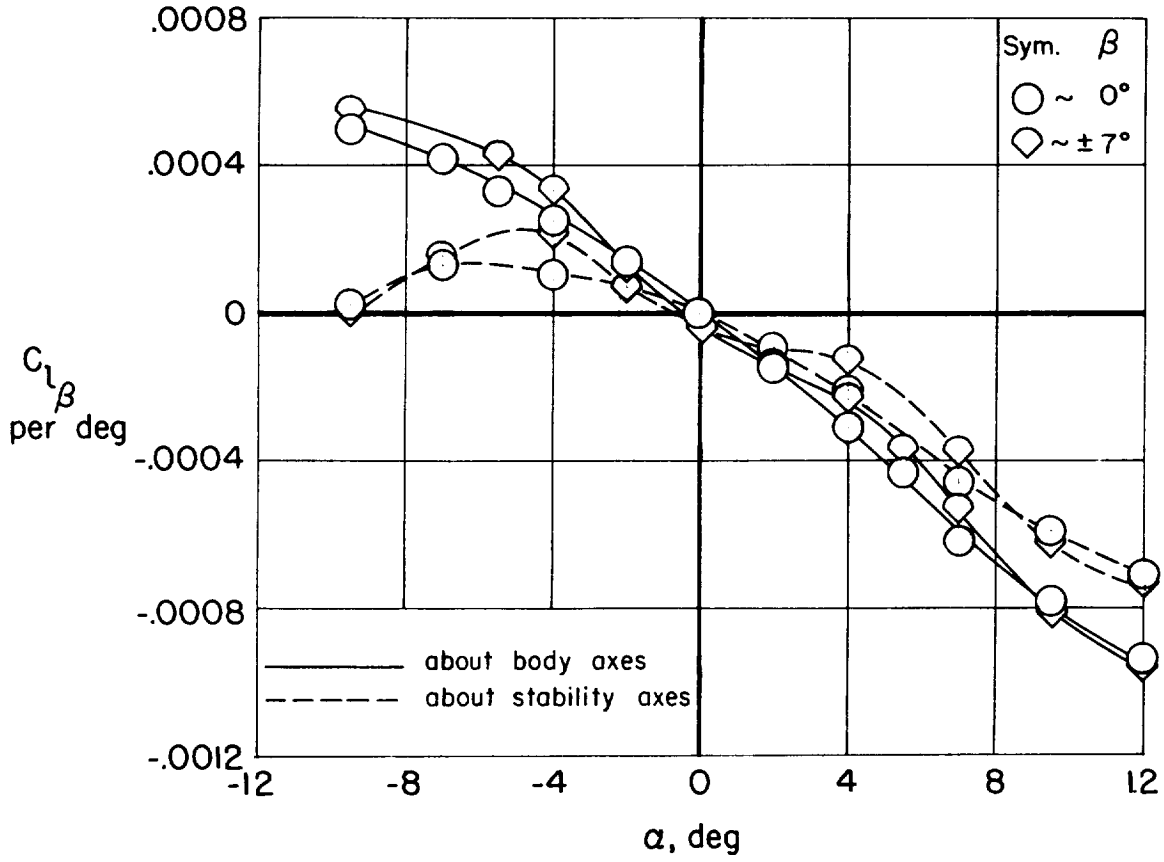

Figure 15.- Variation of rolling-moment-curve slope with angle of attack at two angles of sideslip.

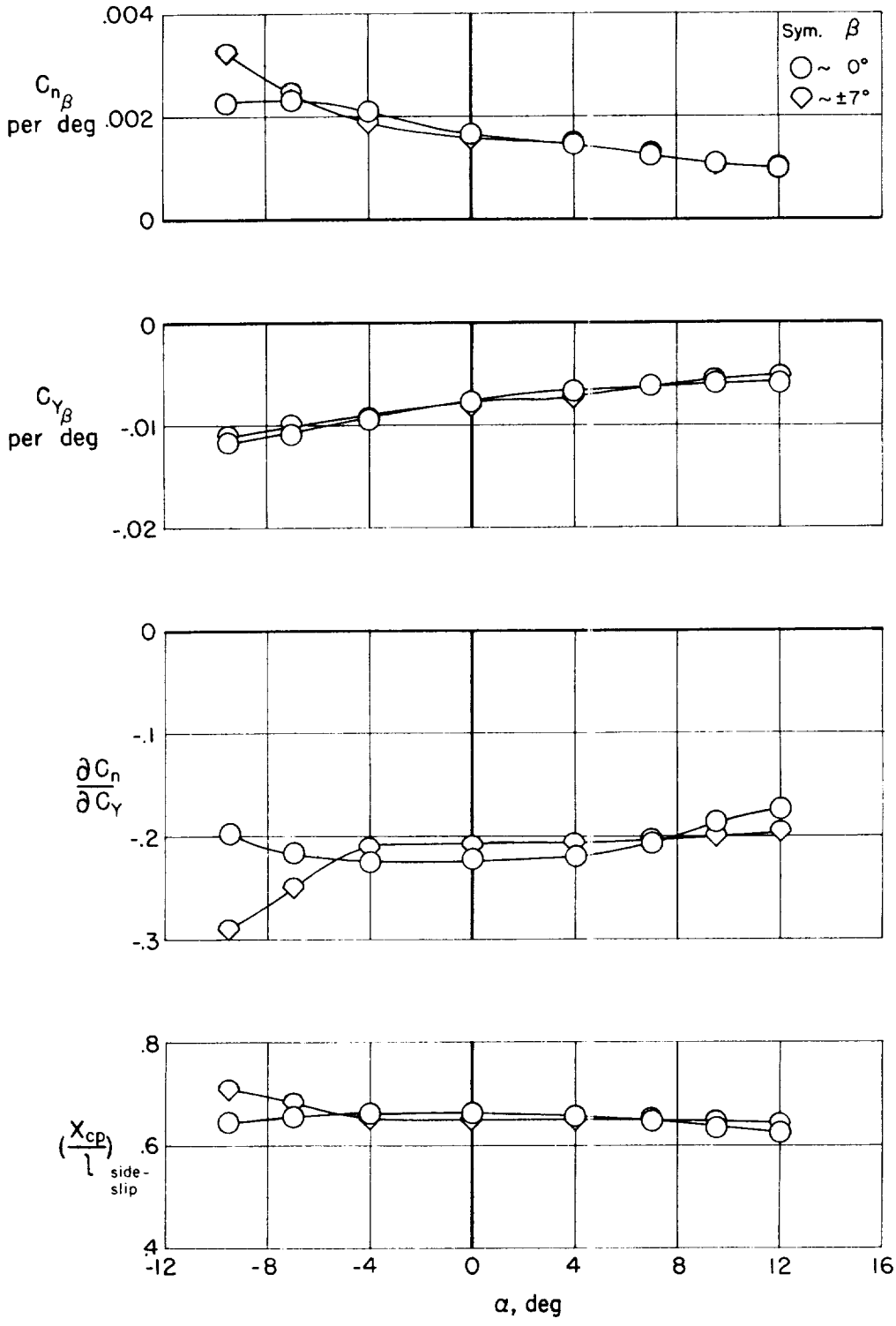

Figure 16.- Variations of directional derivatives and center of pressure with angle of attack at two angles of sideslip.

NASA TN D-330
National Aeronautics and Space Administration.
AERODYNAMIC PERFORMANCE AND STATIC STABILITY AT MACH NUMBER 3.3 OF AN AIRCRAFT CONFIGURATION EMPLOYING THREE TRIANGULAR WING PANELS AND A BODY OF EQUAL LENGTH. Carlton S. James. August 1960. 34p. OTS price, $1.00. (NASA TECHNICAL NOTE D-330)

Wind-tunnel measurements of performance and static stability at combined angles of attack and sideslip were made on a supersonic aircraft configuration at a Mach number of 3.3 and a Reynolds number of 5.46 million. A maximum lift-drag ratio of 6.65 (excluding base drag) was measured at a lift coefficient of 0.100 and an angle of attack of 3.6°. The lift-drag ratio remained greater than 3 to a lift coefficient of 0.35. Estimated performance was in reasonable agreement with experiment. Static stability characteristics were favorable within the test range. Longitudinal and directional centers of pressure were

Copies obtainable from NASA, Washington (over)

I. James, Carlton S.
II. NASA TN D-330

NASA

NASA TN D-330
National Aeronautics and Space Administration.
AERODYNAMIC PERFORMANCE AND STATIC STABILITY AT MACH NUMBER 3.3 OF AN AIRCRAFT CONFIGURATION EMPLOYING THREE TRIANGULAR WING PANELS AND A BODY OF EQUAL LENGTH. Carlton S. James. August 1960. 34p. OTS price, $1.00. (NASA TECHNICAL NOTE D-330)

Wind-tunnel measurements of performance and static stability at combined angles of attack and sideslip were made on a supersonic aircraft configuration at a Mach number of 3.3 and a Reynolds number of 5.46 million. A maximum lift-drag ratio of 6.65 (excluding base drag) was measured at a lift coefficient of 0.100 and an angle of attack of 3.6°. The lift-drag ratio remained greater than 3 to a lift coefficient of 0.35. Estimated performance was in reasonable agreement with experiment. Static stability characteristics were favorable within the test range. Longitudinal and directional centers of pressure were

Copies obtainable from NASA, Washington (over)

I. James, Carlton S.
II. NASA TN D-330

NASA

NASA TN D-330
National Aeronautics and Space Administration.
AERODYNAMIC PERFORMANCE AND STATIC STABILITY AT MACH NUMBER 3.3 OF AN AIRCRAFT CONFIGURATION EMPLOYING THREE TRIANGULAR WING PANELS AND A BODY OF EQUAL LENGTH. Carlton S. James. August 1960. 34p. OTS price, $1.00. (NASA TECHNICAL NOTE D-330)

Wind-tunnel measurements of performance and static stability at combined angles of attack and sideslip were made on a supersonic aircraft configuration at a Mach number of 3.3 and a Reynolds number of 5.46 million. A maximum lift-drag ratio of 6.65 (excluding base drag) was measured at a lift coefficient of 0.100 and an angle of attack of 3.6°. The lift-drag ratio remained greater than 3 to a lift coefficient of 0.35. Estimated performance was in reasonable agreement with experiment. Static stability characteristics were favorable within the test range. Longitudinal and directional centers of pressure were

Copies obtainable from NASA, Washington (over)

I. James, Carlton S.
II. NASA TN D-330

NASA

NASA TN D-330
National Aeronautics and Space Administration.
AERODYNAMIC PERFORMANCE AND STATIC STABILITY AT MACH NUMBER 3.3 OF AN AIRCRAFT CONFIGURATION EMPLOYING THREE TRIANGULAR WING PANELS AND A BODY OF EQUAL LENGTH. Carlton S. James. August 1960. 34p. OTS price, $1.00. (NASA TECHNICAL NOTE D-330)

Wind-tunnel measurements of performance and static stability at combined angles of attack and sideslip were made on a supersonic aircraft configuration at a Mach number of 3.3 and a Reynolds number of 5.46 million. A maximum lift-drag ratio of 6.65 (excluding base drag) was measured at a lift coefficient of 0.100 and an angle of attack of 3.6°. The lift-drag ratio remained greater than 3 to a lift coefficient of 0.35. Estimated performance was in reasonable agreement with experiment. Static stability characteristics were favorable within the test range. Longitudinal and directional centers of pressure were

Copies obtainable from NASA, Washington (over)

I. James, Carlton S.
II. NASA TN D-330

NASA

close to the respective centroids of projected planform and side area.

(Initial NASA distribution: 1, Aerodynamics, aircraft; 3, Aircraft; 50, Stability and control.)

Copies obtainable from NASA, Washington

NASA

NASA TN D-330

close to the respective centroids of projected planform and side area.

(Initial NASA distribution: 1, Aerodynamics, aircraft; 3, Aircraft; 50, Stability and control.)

Copies obtainable from NASA, Washington

NASA

NASA TN D-330

close to the respective centroids of projected planform and side area.

(Initial NASA distribution: 1, Aerodynamics, aircraft; 3, Aircraft; 50, Stability and control.)

Copies obtainable from NASA, Washington

NASA

NASA TN D-330

close to the respective centroids of projected planform and side area.

(Initial NASA distribution: 1, Aerodynamics, aircraft; 3, Aircraft; 50, Stability and control.)

Copies obtainable from NASA, Washington

NASA

NASA TN D-330
National Aeronautics and Space Administration.
AERODYNAMIC PERFORMANCE AND STATIC STABILITY AT MACH NUMBER 3.3 OF AN AIRCRAFT CONFIGURATION EMPLOYING THREE TRIANGULAR WING PANELS AND A BODY OF EQUAL LENGTH. Carlton S. James. August 1960. 34p. OTS price, $1.00. (NASA TECHNICAL NOTE D-330)

Wind-tunnel measurements of performance and static stability at combined angles of attack and sideslip were made on a supersonic aircraft configuration at a Mach number of 3.3 and a Reynolds number of 5.46 million. A maximum lift-drag ratio of 6.65 (excluding base drag) was measured at a lift coefficient of 0.100 and an angle of attack of 3.6°. The lift-drag ratio remained greater than 3 to a lift coefficient of 0.35. Estimated performance was in reasonable agreement with experiment. Static stability characteristics were favorable within the test range. Longitudinal and directional centers of pressure were

Copies obtainable from NASA, Washington (over)

I. James, Carlton S.
II. NASA TN D-330

NASA

NASA TN D-330
National Aeronautics and Space Administration.
AERODYNAMIC PERFORMANCE AND STATIC STABILITY AT MACH NUMBER 3.3 OF AN AIRCRAFT CONFIGURATION EMPLOYING THREE TRIANGULAR WING PANELS AND A BODY OF EQUAL LENGTH. Carlton S. James. August 1960. 34p. OTS price, $1.00. (NASA TECHNICAL NOTE D-330)

Wind-tunnel measurements of performance and static stability at combined angles of attack and sideslip were made on a supersonic aircraft configuration at a Mach number of 3.3 and a Reynolds number of 5.46 million. A maximum lift-drag ratio of 6.65 (excluding base drag) was measured at a lift coefficient of 0.100 and an angle of attack of 3.6°. The lift-drag ratio remained greater than 3 to a lift coefficient of 0.35. Estimated performance was in reasonable agreement with experiment. Static stability characteristics were favorable within the test range. Longitudinal and directional centers of pressure were

Copies obtainable from NASA, Washington (over)

I. James, Carlton S.
II. NASA TN D-330

NASA

NASA TN D-330
National Aeronautics and Space Administration.
AERODYNAMIC PERFORMANCE AND STATIC STABILITY AT MACH NUMBER 3.3 OF AN AIRCRAFT CONFIGURATION EMPLOYING THREE TRIANGULAR WING PANELS AND A BODY OF EQUAL LENGTH. Carlton S. James. August 1960. 34p. OTS price, $1.00. (NASA TECHNICAL NOTE D-330)

Wind-tunnel measurements of performance and static stability at combined angles of attack and sideslip were made on a supersonic aircraft configuration at a Mach number of 3.3 and a Reynolds number of 5.46 million. A maximum lift-drag ratio of 6.65 (excluding base drag) was measured at a lift coefficient of 0.100 and an angle of attack of 3.6°. The lift-drag ratio remained greater than 3 to a lift coefficient of 0.35. Estimated performance was in reasonable agreement with experiment. Static stability characteristics were favorable within the test range. Longitudinal and directional centers of pressure were

Copies obtainable from NASA, Washington (over)

I. James, Carlton S.
II. NASA TN D-330

NASA

NASA TN D-330
National Aeronautics and Space Administration.
AERODYNAMIC PERFORMANCE AND STATIC STABILITY AT MACH NUMBER 3.3 OF AN AIRCRAFT CONFIGURATION EMPLOYING THREE TRIANGULAR WING PANELS AND A BODY OF EQUAL LENGTH. Carlton S. James. August 1960. 34p. OTS price, $1.00. (NASA TECHNICAL NOTE D-330)

Wind-tunnel measurements of performance and static stability at combined angles of attack and sideslip were made on a supersonic aircraft configuration at a Mach number of 3.3 and a Reynolds number of 5.46 million. A maximum lift-drag ratio of 6.65 (excluding base drag) was measured at a lift coefficient of 0.100 and an angle of attack of 3.6°. The lift-drag ratio remained greater than 3 to a lift coefficient of 0.35. Estimated performance was in reasonable agreement with experiment. Static stability characteristics were favorable within the test range. Longitudinal and directional centers of pressure were

Copies obtainable from NASA, Washington (over)

I. James, Carlton S.
II. NASA TN D-330

NASA

close to the respective centroids of projected planform and side area.

(Initial NASA distribution: 1, Aerodynamics, aircraft; 3, Aircraft; 50, Stability and control.)

NASA TN D-330

close to the respective centroids of projected planform and side area.

(Initial NASA distribution: 1, Aerodynamics, aircraft; 3, Aircraft; 50, Stability and control.)

Copies obtainable from NASA, Washington

NASA

NASA TN D-330

close to the respective centroids of projected planform and side area.

(Initial NASA distribution: 1, Aerodynamics, aircraft; 3, Aircraft; 50, Stability and control.)

Copies obtainable from NASA, Washington

NASA

NASA TN D-330

close to the respective centroids of projected planform and side area.

(Initial NASA distribution: 1, Aerodynamics, aircraft; 3, Aircraft; 50, Stability and control.)

Copies obtainable from NASA, Washington

NASA